**The People's Democratic Republic of Algeria**

**Ministry of Higher Education and Scientific Research**

**Higher normal school of Technological Education**

**- Skikda -**

**Department:** Technology

**Major:** Mechanical Engineering

**Graduation Thesis for Obtaining the Secondary Education Teacher's Certificate**

# Numerical Study of Forced Convection in an Inclined Tube Using a Vortex Generator


**Prepared by:**

- Beddiar Kaouther
- Hadji Aridj

**Under the supervision of the professor**:

- Mrs. Merimeche Imene


| **Examination Committee:** | **Rank :** |
|---|---|
| **Discussing:** Mrs.Bouhali Rima. | Professor Lecturer B. |
| **Perisident:** Mr.BenSanaa Toufik. | Professor Lecturer A. |
| **Supervisor:**Mrs.Merimeche Imene . | Professor Lecturer B. |

**Academic year: 2023/2024**

**Thanks**

**F**irst of all, I thank ALLAH for giving me the strength and will to accomplish this humble work .

**T**hank you to my supervisor **Mrs. MERIMECHE.I** for taking care of our work and providing

her valuable advice and, above all her patience with us.

**I** thank **Mr. RAHMOUNI** the head of the Technology Department, for all the services he has provided us over the past five years and for helping us reach this special day. He has my utmost gratitude and appreciation.

**I** offer my sincere respect and thanks to the members of **The jury Mrs.BOUHALI .R and Mr.BENSANAA .T** who approved the evaluation of our work.

**M**y thanks are also addressed to my **dear parents**, for their love, their sacrifices and their patience .

**I** would like to thank all my teachers who took care of our formation and training throughout the academic course so that we can stand here today .

I thank my colleague and partner in the preparation of this work **HAJI ARIDJ** for her effort and encouragement to us.

**I** would like to thank everyone who contributed, whether active or non-active, in achieving this work that they fined here is an expression of my sincere

gratitude and my sincere thanks .

**Gifts**

**I** dedicate this thesis

**T**o my dearest parents

**T**o my brothers and sisters

**T**o all my familly

**T**o alla my friends dhikra, aridj and chourouk

**Kaouther Beddiar**

**Thanks**

At the outset of my speech, I must first express my gratitude to Allah, who has enabled me to reach this high academic stage, and paved the way for me to be among you today.

Furthermore, I would like to express my deep gratitude to **Mrs. MERIMECHE.I** for supervising this dissertation.

I had the pleasure of working under your guidance. I appreciate your kindness and spontaneity with which you led this work, as well as your availability and advice which helped me improve my work.

And i like to thank **Mr.RAHMOUNI** the head of the Technology Department, for his guidnace and support in all this 5 years your leadership is greatly appreciated.

I offer this success to :

My dear **parents**,

No matter what I say or do, I never seem to be able to thank you enough. It is thanks to your encouragement, kindness, and presence by my side that I have achieved this respectful journey.

I hope that you are proud of me, and that I have been able to live up to the hopes you have placed in me.

My dear brothers, **RIM, MOUIZ, RIHAB** Thank you for your moral support, your trust, and your valuable advice, which have helped me in difficult times.

I am grateful to my friend **Beddiar Kaouther** who was by my side to achieve this work and for her moral support throughout this period.

And all my friends, **SARA, KAWTHER, MIMI**.

Through these lines, I cannot describe all my feelings of love, the only word I can say is thank you, truly thank you very much to everyone who has contributed to the completion of this thesis.

**Hadji Aridj**

**Summary**

In our research, we conducted a numerical study to enhance heat transfer using forced convection in various pipes (horizontal, inclined at 30 degrees, and 60 degrees) employing vortex generators. We chose water as the fluid for our study and utilized Gambit for mesh generation, setting boundary conditions, and Fluent for simulation and analysis. The results showed that the optimal configuration ensuring optimal heat flux was an inclined pipe at a 30 degree angle with a swirl generator at 50 mm.

**تلخيص**

قمنا في بحثنا بدراسة عددية لتحسين انتقال الحرارة بواسطة الحمل الحراري القسري في مختلف الانابيب (انبوب افقي ,مائل ب 30درجة و 60درجة ) باستعمال مولدات الدوامة ,باختيار الماء كالمائع في دراستنا واعتمدنا على برنامج غامبيت للرسم الشبكة المدروسة وتحديد الشروط الحدودية وبرنامج فلونت للمحاكاة والتحليل ,فكانت النتائج كالاتي ان احسن تركيب يضمن تدفق حراري امثل هو انبوب مائل بزاوية 30درجة مع مولد دوامة عند 50 مم.

**Résumé**

Dans notre recherche, nous avons mené une étude numérique pour améliorer le transfert de chaleur par convection forcée dans différents types de tuyaux (horizontal, incliné à 30 degrés et 60 degrés) en utilisant des générateurs de tourbillons. Nous avons choisi l'eau comme fluide pour notre étude et avons utilisé Gambit pour la génération du maillage, la définition des conditions aux limites, ainsi que Fluent pour la simulation et l'analyse. Les résultats ont montré que la meilleure configuration assurant un flux thermique optimal était un tuyau incliné à 30 degrés avec un générateur de tourbillon à 50 mm.

Table des matières

## List Of Figures

## List of Tables

## NOMENCLATURE

| | | |
|---|---|---|
| $\rho$ | The mass volume | $[kg/m^3]$ |
| M | The mass | [kg ] |
| V | The volume | $[m^3]$ |
| P | The absolute pressure | $[N/m^2]$ |
| R | The general constant of gases | $[R = 287\ J/kg\,.K]$ |
| T | The absolute temperature | [K] |
| D | The density of gases | $[kg\ /m^3]$ |
| T | Shear stress | $[N/\ m^2]$ |
| F | Applied force | [N] |
| A | Contact area | $[\ m^2]$ |
| $\mu$ | Dynamic viscosity | $\left[N.\frac{s}{m2}\right] = [Pa.s]$ |
| $\vartheta$ | Kinematic viscosity | $[m^2/s]$ |
| Cp | Specific heat by mass at constant pressure | $[j.kg^{-1}.k^{-1}]$ |
| $R_e$ | Reynolds number. | / |
| $T_S$ | Surface temperature. | [K] |
| $T_\infty$ | Fluid temperature . | [K] |
| k | Thermal conductivity. | [W/m· K] |
| $\dot{q}_{conv}$ | convective heat transfer rate. | $[W.m^{-2}]$ |
| $\dot{q}_{cond}$ | Conduction heat transfer rate. | $[W.m^{-2}]$ |
| H | The convective heat transfer coefficient. | $[W\ /m^2.K]$ |
| $\tau_s$ | The shear stress . | $[N/m^2]$ |
| M | The dynamic viscosity of the fluid . | [ kg/m.s or $N.s/m^2$] |
| $C_f$ | Skin friction coefficient. | / |
| Nu | Nusselt number. | / |
| Pr | Prandtl number . | / |
| $C_P$ | Specific heat capacity. | [J/kg.K] |
| A | Thermal diffusivity. | $[m^2/s]$ |
| Gr | Grashof number. | / |
| G | Gravitaional acceleration. | $[m/s^2]$ |
| $\beta$ | Coefficient of volume expansion. | [1 /K] |
| $\delta$ | Characteristic lenghth of the geometry | [m] |
| $\dot{m}$ | The mass flow rate. | [kg/s] |

| | | |
|---|---|---|
| $\mathbf{A_c}$ | The cross-sectional area. | **[ $m^2$]** |
| $\mathbf{L_h}$ | The hydrodynamic entry length. | **[m]** |
| $\mathbf{L_t}$ | The thermal entry length . | **[m]** |
| $\mathbf{T_i}$ | Mean fluid temperature at the tube inlet. | **[K=°C+273]** |
| $\mathbf{T_e}$ | Mean fluid temperature at the tube exit. | **[K=°C+273]** |
| $\mathbf{\dot{q}_s}$ | Constant surface heat flux rate. | $[\mathbf{W.m^{-2}}]$ |
| $\mathbf{h_x}$ | The local heat transfer coefficent. | **[$W/m^2.K$]** |
| $\mathbf{V_{avg}}$ | The average velocity. | **[m/s]** |
| $\mathbf{u(r)}$ | The velocity profile. | **[m/s]** |
| $\mathbf{\dot{E}_{fluid}}$ | The rate of energy conversion in the fluid. | **[J /s]=[W]** |
| $\mathbf{Nu_x}$ | The local nusselt number. | / |
| $\mathbf{Re_x}$ | The local Reynolds number. | / |
| $\boldsymbol{\eta}$ | Thermal enhancement factor. | / |
| $\mathbf{Nu_o}$ | Nusselt number for the plain tube. | / |
| $\mathbf{\dot{S}_{gen}}$ | The rate of entropy generation. | **[W/K]** |
| $\mathbf{\Delta T}$ | The temperature difference across the tube ends. | **[K=°C+273]** |
| $\mathbf{U}$ | The mean velocity. | **[m/s]** |
| $\mathbf{m_{in}}$ | Total mass entering. | **[kg]** |
| $\mathbf{m_{out}}$ | Total mass leaving. | **[kg]** |
| $\mathbf{m_{sys}}$ | The mass of the system. | **[kg]** |
| $\mathbf{\dot{V}}$ | The volume flow rate . | **[$m^3/s$]** |
| **Cv** | The specific heat at constant volume. | **[J/kg·K]** |
| $\mathbf{E_{in}}$ | Total energy entering in the system. | **[J]** |
| $\mathbf{E_{out}}$ | Total energy leaving the system. | **[J]** |
| $\mathbf{\Delta E_{sys}}$ | Changing in the total energy in the system. | **[J]** |
| $\mathbf{\dot{E}_{in}}$ | The rate of Total energy entering in the system. | **[J /s]=[W]** |
| $\mathbf{\dot{E}_{out}}$ | The rate of Total energy leaving the system. | **[J /s]=[W]** |
| $\mathbf{\Delta U_{system}}$ | The change in its internal energy. | **[J]** |
| **Q** | Heat. | **[J]** |
| **W** | Work. | **[J]** |
| $\mathbf{\dot{Q}}$ | The rate of net heat transfer. | **[J /s]=[W]** |
| $\mathbf{\vec{F}}$ | External force. | **[N]** |
| $\mathbf{\sum \vec{F}}$ | Total force acting on control volume. | **[N]** |
| $\mathbf{d\vec{F}_{gravity}}$ | Gravitational force acting on a fluid element . | **[N]** |
| $\mathbf{\sum \vec{F}_{body}}$ | Total body force acting on control volume. | **[N]** |
| $\mathbf{V_r}$ | Mass flow rate at all locations. | **[kg/s]** |

| | | |
|---|---|---|
| $\boldsymbol{\varphi_p, \varphi_E, \varphi_w}$ | Electric potential at node P ,E,W on the order . | **[V]** |
| $\boldsymbol{(\delta x)_E}$ | The distance between nodes P and E. | **[m]** |
| $\boldsymbol{(\delta x)_w}$ | The distance between nodes w and P. | **[m]** |
| $\boldsymbol{\Delta x}$ | Finite volume length. | **[m]** |
| $\boldsymbol{h = \frac{b-a}{n}}$ | Length of each subinterval . | **[m]** |
| **N** | The number of subintervals. | / |
| $\boldsymbol{\mu_t}$ | The proportionality constant representing turbulent viscosity . | **[kg/m·s]=[ Pa·s]** |
| $\boldsymbol{G_k}$ | Represents the generation of turbulent kinetic energy due to gradients in the mean velocity. | **[W/kg]** |
| $\boldsymbol{G_b}$ | The generation of turbulent kinetic energy resulting from turbulence dissipation. | **[W/kg]** |
| $\boldsymbol{C_{1\varepsilon}}$ ; $\boldsymbol{C_{2\varepsilon}}$; $\boldsymbol{C_{3\varepsilon}}$ | Empirical constants. | / |
| $\boldsymbol{\sigma_k}$ **et** $\boldsymbol{\sigma_\varepsilon}$ | Prandtl numbers for k and ε respectively. | / |
| $\boldsymbol{S_k, S_\varepsilon}$ | Source terms. | / |
| $\boldsymbol{C_\mu}$ | Empirical constant. | / |

# General Introduction

## General Introduction

The objectives of this work Which focuses on improving heat transfer using forced convection in inclined pipes with vortex generators, can be summarized as follows:

1. Enhancing heat transfer efficiency: Vortex generators contribute to improving fluid flow inside the pipes, leading to increased heat transfer efficiency. The swirling action enhances fluid agitation and circulation, thus promoting heat exchange between the fluid and the pipe walls.

2. Flow direction and control: Vortex generators can be used to direct flow in a specific manner inside the pipe, allowing for improved heat distribution and avoiding temperature stratification phenomena within the pipes.

3. Reducing heat losses: By enhancing fluid movement and improving temperature distribution, vortex generators can reduce heat losses and enhance pipe efficiency as a means of heat transfer.

4. Multiple technical applications: Vortex generators enable the improvement of performance in various technical applications that require efficient heat transfer, such as heat exchangers, cooling systems, and thermal pipes.

In general, studying heat transfer in inclined pipes using vortex generators enhances our understanding of heat transfer processes and enables us to improve the efficiency of those processes in various applications.

**Chapter I:** This chapter discusses the dynamic realm of fluid mechanics, covering fluid properties and classification to select the most suitable fluid based on our study. It explores the fundamental principles governing fluid behavior, flow patterns, and heat transfer mechanisms essential for designing and optimizing various engineering systems. Additionally, it reviews previous studies related to enhancing both passive and active heat transfer rates. One of the key innovations discussed in this chapter, crucial for our study on enhancing heat transfer, is the integration of vortex generators.

**Chapter II:** This chapter discusses the numerical method for finite volumes. The geometry, meshing, and boundary conditions are determined using a preprocessor named "Gambit," while simulation parameters are set at the "Fluent," processor level. Based on the obtained results, it emphasizes the importance of choosing a suitable mesh for accurate results and compares Fluent's results with empirical relations and experiments to conclude that Fluent is an excellent choice for accurately simulating heat transfer problems.

**Chapter III:** In this chapter, we present and discuss the simulation results of thermal convection in horizontal cylindrical geometry and two pipes at different inclinations ($\alpha = 30°, 60°$) with and without control elements at three different positions (x = 50, 200, and 400 mm). Additionally, we analyze the results of the pipe with a control element at x = 50 mm to achieve optimal design by determining the Nusselt number.

Finally, this thesis will conclude with a general conclusion.

# CHAPTER I
# BIBLIOGRAPHY

## I-1- Introduction

In this chapter, we delve into the dynamic realm of fluid mechanics, where the study of fluids materials that continuously deform under applied shear stress is of paramount importance.

This chapter explores the fundamental principles that govern fluid behavior, flow patterns, and heat transfer mechanisms, which are essential for designing and optimizing countless engineering systems, from heating, ventilation, and air conditioning units to spacecraft.

We have mentioned some methods for enhancing both passive and active heat transfer rates through an understanding of the nuances in fluid dynamics and forced (such as pump and fan) and natural convection.

We have focused on internal forced convection in tubes and the developments of velocity and temperature in the entrance region and the fully developed, in addition to the key parameters and dimensionless numbers used along with some common correlations for the Nusselt number related to laminar and turbulent systems in tubes.

One of the innovations we have discussed, which has garnered significant attention for its potential to revolutionize heat exchanger performance, is the integration of vortex generators. These devices work to enhance heat transfer through two techniques: boundary layer disruption or increased surface area.

Engineers now have the ability to predict how fluids interact with their surroundings under different conditions, leading to innovations in technology and improvements in efficiency across multiple industries.

**I -2-Definition of fluid**

No matter how little the shear stress, a fluid is a material that always deforms when a tangential shear force is applied.

Consequently, the liquid and gas (or vapor) phases of the physical forms that matter resides in are considered fluids[1].

If you compare the behavior of fluids and solids, you will see that there is an obvious difference between the fluid and solid states of matter. When a shear force is applied, a solid deforms, yet this deformation does not get worse with time[2].

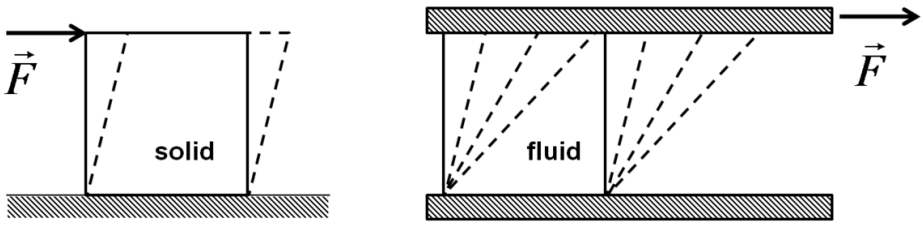


*Figure (I.1): Deformation of solid versus deformation of fluid.*

**Remark :**

We mentioned that there are many types of fluids :

**I-2-1-Ideal fluid**

This type of fluid does not have viscosity; specifically, this type cannot exist because all fluids have some viscosity) [4].

**I-2-2-Real fluid**

A real fluid is one that has viscosity, surface, tension, and compressibility in addition to density. The real fluids are actually available in nature [5].

**I-2-3-Newtonian fluid**

Any fluid that abides by Newton's law of viscosity is known as a Newtonian fluid, for example, hydrogen and water [5].

**I-2-4-Non-Newtonian fluid**

Category of fluids for which the viscosity is not independent of the rate of shear, and they are called non-Newtonian fluids [1].

The meaning of it increasing fluids resistance with increasing strainrate. Examples:gelatine, oobleck (made from corn strach and water) [6].

**I-2-5-Compressible Fluid**

If the density changes in a process and this change must be taken into account, the flow fluid is called compressible flow [7].

The most common example of a compressible flow fluid concerns the flow of gases [8].

**I-2-6-Incompressible Fluid**

If the density of a fluid does not change in a process of heat transfer, the flow of fluid is accepted as an incompressible flow [7].

Where the flow of liquids may frequently be incompressible [8].

**I-3-Properties of fluids**

**I-3-1-The mass volume**

Is defined as the ratio of the mass of a given amount of a substance to the volume that this amount occupies [1].

denoted by ρ (lowercase Greek rho).

$$\rho = \frac{m}{v} \qquad (I.1)$$

Where :

ρ: Density.

m: The mass.

v: The volume.

**In SI unites**

mass in kg and volume in $m^3$, so the units of density are kg /$m^3$ .

For example [6]:

The density of water at a temperature of 4°C is equal to 1000 kg/$m^3$ .

The heaviest common liquid is mercury, and the lightest gas is hydrogen. Compare their

densities at 20°C and 1 atm:

Mercury: ρ= 13,580 kg/$m^3$ Hydrogen: ρ= 0.0838 kg/$m^3$

**Important notice**

To calculate the density of gases, we use the general law of ideal gases [1]:

$$P \times v = m \times R \times T \qquad (I.2)$$

The density of gases:

$$\rho = \frac{P}{RT} \quad (I.3)$$

**Where :**

P: Absolute pressure $[N/m^2]$.

R: General constant of gases $[R = 287\ J/kg\,.K]$.

T: Absolute temperature [K].

D: Density of gases $[kg/m^3]$.

**I-3-2 Viscosity**

Is the amount of internal friction force between the layers of the fluid during flow, and it is also a measure of the resistance of the fluid to shear and deformation [6].

The frictional force in the fluid results from the cohesion and exchange of the amount of motion between the molecules in the fluid [6].

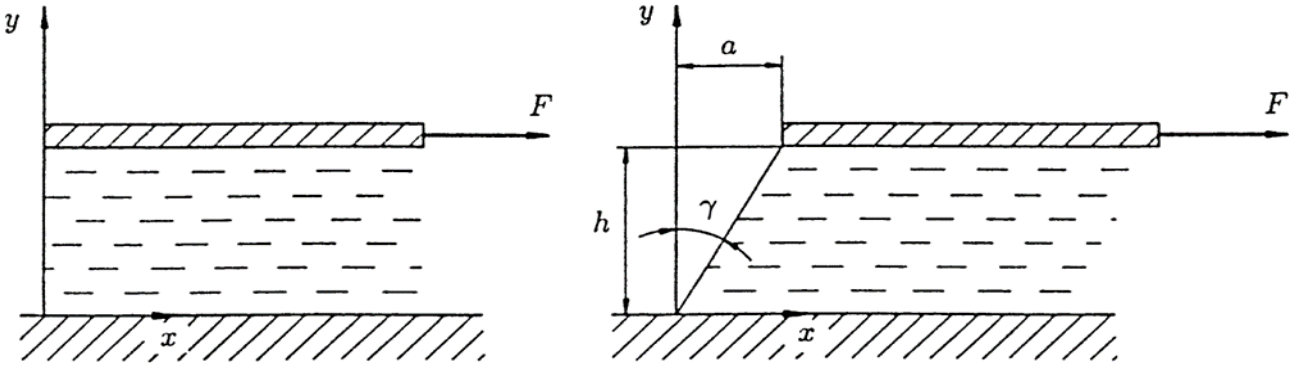


*Figure (I.2): The experiment of setting the viscosity of the fluid [9].*

From the figure (I.3) we have a shear stress :

$$\tau = \frac{F}{A} \quad (I.4)$$

F :Applied force [N].
A : Contact area $[m^2]$.

And also, the shear stress is the ratio of the change in speed relative to the change in distance between the two plates multiplied by the viscosity.

$$\tau = \mu \frac{dU}{dy} \quad (I.5)$$

Where (μ) is the constant of proportionality, it is known as dynamic viscosity, expressed in accordance with the law [6].

$$\mu = \frac{\tau}{dU/dy} \quad (I.6)$$

The viscosity units are : $\left[\mathrm{N}.\frac{\mathrm{s}}{\mathrm{m}^2}\right] = [\mathrm{Pa}.\mathrm{s}]$

The ratio between dynamic viscosity and density is known as kinematic viscosity.

$$\vartheta = \frac{\mu}{\rho} \qquad (I.7)$$

Its unity $[\mathrm{m}^2/\mathrm{s}]$.

**I-3-3 Thermal conductivity**

It's defined as the spontaneous transfer of thermal energy through matter from one zone of high temperature to another with a lower temperature than the previous one to reach thermal homogeneity [10].

Thermal conductivity occurs through molecular agitation and contact; and does not result in the bulk movement of the solid itself, heat moves along a temperature gradient [10].

Thermal conductivity is measured in watts per meter.kelvin ($W.m^{-1}.k^{-1}$) [11].

**Example :**

Water: 0.607 at 25 °C ($W.m^{-1}.k^{-1}$).

Ethanol: 0.169 at 25 °C ($W.m^{-1}.k^{-1}$).

**I-3-4 specific heat by mass at constant pressure**

The specific heat of a fluid at constant pressure is defined as the quantity of heat required to raise the temperature of the unit mass of the fluid by 1 degree, with the pressure remaining constant during heating.

It is given by the symbol Cp ($\mathrm{j}.\mathrm{kg}^{-1}.\mathrm{k}^{-1}$) [12].

**Example :**

Air:1005($\mathrm{j}.\mathrm{kg}^{-1}.\mathrm{k}^{-1}$).

Watter: 4180($\mathrm{j}.\mathrm{kg}^{-1}.\mathrm{k}^{-1}$).

**I-4 classification of fluid flow**

Fluid flow is a part of fluid mechanics and deals with fluid dynamics, it involves the motion of a fluid subjected to unbalanced forces. This motion continues as long as unbalanced forces are applied [8].

### I -4-1 Fluid Statics versus Fluid Dynamics

#### A-Fluid statics

Is the part of fluid mechanics that deals with fluids when there is no relative motion between the fluid particles. Typically, this includes two situations: when the fluid is at rest and when it moves like a rigid solid (commonly referred to as hydrostatics) [6].

#### B-Fluid dynamics

Is the study of fluids in motion where fluid dynamics of liquids is called hydrodynamics and of compressible gases is called gas dynamics [6].

### I-4-2 Unsteady versus Steady Flow

#### A- Steady flow

When the heat transfer process does not depend on time, it is called a steady state. In this state, temperature, pressure, or speed do not change with time [7].

#### B- Unsteady flow

When the dependent variable of a heat transfer problem, such as temperature, pressure, or velocity, changes with time, the heat transfer process is called unsteady state or transient heat transfer [7].

### I -4-3 Laminar versus turbulent flow

#### A-laminar flow

At low speeds, fluid particles move smoothly, and the velocity, pressure, and other flow properties at each point in this fluid remain constant. Laminar flow over a horizontal surface may be thought of as consisting of thin layers.

The fluid in contact with the horizontal surface is stationary, but all other layers slide over each other with different velocities [1].

#### B-Turbulent flow

At higher speeds, fluid particles begin to exhibit random fluctuations and move in a chaotic manner. A turbulent flow refers to an irregular flow in which eddies and flow instabilities occur; it is in contrast to the laminar regime. The turbulence regime is extremely frequent in natural phenomena and engineering applications; some examples: the rise of cigarette smoke, blood flow in arteries [1].

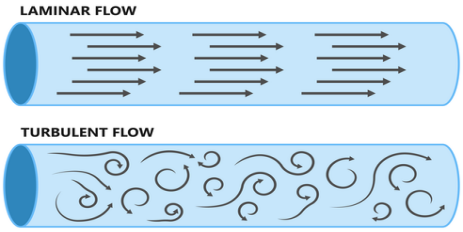


*Figure (I.3) :Laminer and Turbulent flow [8].*

### I-4-4 Incompressible versus Compressible Flow

### A- Incompressible Flow

In an incompressible flow, the volume of a given fluid parcel does not change (compress). This implies that density is uniform throughout the fluid. It is a reasonable assumption for all liquid flows and low-speed gas flows [14].

For many liquids, density is only a weak function of temperature at modest pressure, at high pressure, compressibility effects in liquids can be important. Pressure and density changes in liquids cause they are related by the bulk compressibility modulus or modulus of elasticity [8].

### B-Compressible Flow

In a compressible flow, the volume of a given fluid can change with pressure. Compressible flows are further classified according to the speed of the fluid relative to the speed of sound waves. This ratio is non-dimensional and is called the Mach number (Ma) [8].

### I-4-5 viscous and inviscid

### A-viscous

Fluid moves in adjacent layers without no-slip conition, and it occurs at low velocity when shear stresses are of small magnitude . In another way, it's the fluid that has more resistance to flow [15].

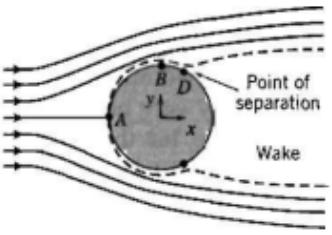


*Figure (I.4): Viscous flow [8].*

2

**B-inviscid**

Is characterized by the random, unpredictable motion of fluid particles, which results in eddy currents. This one occurs at high velocities where the shear stresses are much greater than the viscous one.

In another way, we say the fluid has more resistance or zero resistance to internal friction [16].

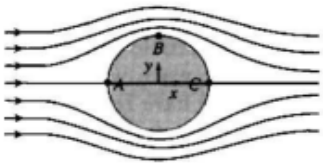


*Figure (I.5): Inviscid flow [8].*

**I-4-6 External Flow and Internal Flow**

**A- Internal Flow**

Is surrounded by solid boundaries that can restrict the development of its boundary layer, for example, flow in pipes, duct enclosures, nozzles, etc [1]**.**

**B-external flow**

Flow over bodies immersed in an unbounded fluid so that the flow boundary layer can grow freely in any direction, for example, over aircraft, projectiles, or ground vehicles [5].

**I-5 The convection**

Convection is the transfer of heat from the hotter parts of a liquid or gas to its colder parts by the motion of free particles. The transfer of heat by convection can take place only in liquids and gases and cannot take place in solids because the particles in the solids are fixed at a place and hence cannot move freely [17].

And the convection is classified into:

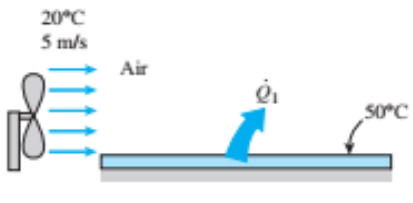


*Figure (I.6): Forced convenction [18].*


*Figure (I.7): Natural convenction [18].*

### I-5-1 Forced convection

Forced convection is a special type of heat transfer through a fluid in the presence of fluid bulk, depending on how the fluid motion is initiated, and the fluid is forced to flow over a surface or in a tube by external means such as a pump or fan [19].

**Mechanism of forced convection**

The fluid motion enhances heat transfer (the higher the velocity, the higher the heat transfer rate).

The rate of convection heat transfer is expressed by Newton's law of cooling [17]:

$$\dot{q}_{conv} = h(T_s - T_\infty) \quad (I.8)$$

h: The convective heat transfer coefficient.

$T_S$: Surface temperature, $T_\infty$ :Fluid temperature.

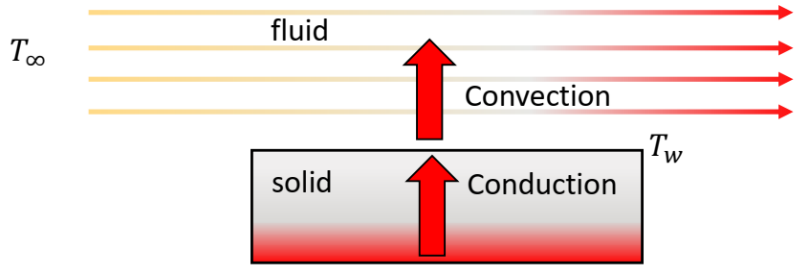


*Figure (I.8): Forced convenction [20].*

We know that the velocity of the fluid layer adjacent to the wall is zero (we called this case the no-slip condition), and from this, the heat transfer between the solid space and this layer is done by thermal conductivity, and we apply Fourier's law to it [17]:

$$\dot{q}_{cond} = -k\frac{\partial T}{\partial y}|_{y=0} \quad (I.9)$$

Then:

$$\dot{q}_{conv} = \dot{q}_{cond} \Longrightarrow h = \frac{-k}{(T_S - T\infty)}\frac{\partial T}{\partial y}|_{y=0} \quad (I.10)$$

And we know that $\dot{q}_{conv} = h(T_s - T_\infty)$ .

#### I-5-1-1 Velocity Boundary Layer

Can be considered a fluid flowing over a space at a velocity $U_\infty$ and temperature$T_\infty$, and the fluid is composed of contigiuous layers.

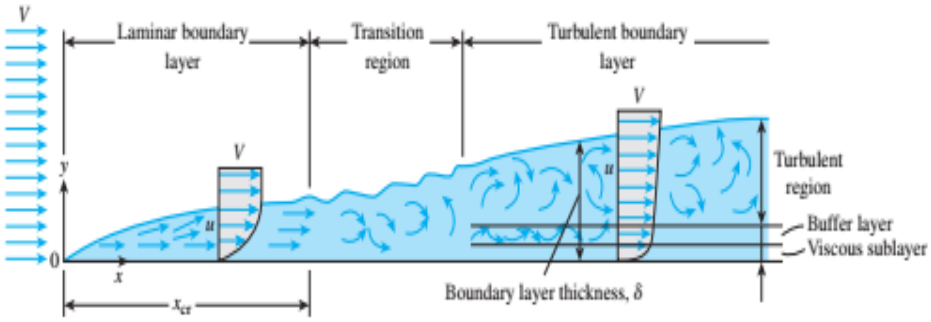


*Figure (I.9): Velocity boundray layer [18].*

We take a non-slip condition on the surface, and the flow proceeds at a speed $U_\infty$ until it reaches a point x = 0. We observe the velocity change from [$U_\infty$ to 0], and this is due to the viscosity between the surface and the fluid layer adjacent to the surface. This layer acts by obstructing the next layer of the fluid. As a result, the velocity value changes by decreasing in the direction (-y) to zero. This phenomenon is called movement retention, and its value decreases in the (y) direction to almost zero as the velocity becomes $U_\infty$.

The area below the on (Figure I.9) is called the velocity boundary layer. It is characterized by the presence of viscous forces inside and absent outside.

The friction between two adjacent acts similar to a drag force (friction force). The drag force per unit area is called the shear stress [18].

$$\tau_s = \mu \left(\frac{dU}{dy}\right)_{y=0} \quad [N/m^2] \qquad (I.11)$$

μ: The dynamic viscosity of the fluid [ kg/m.s or $N.s/m^2$].

The surface shear stress can also be determined from:

$$\tau_s = C_f \times A \frac{dU^2}{2} \quad [N/m^2] \qquad (I.12)$$

We can note three stages of development for the flow:

1. The first stage is laminar flow, where it starts in the boundary layer in a smooth and simplified manner.

2. The second stage is the zone of transition of the flow from laminar to turbulent.

3. The third stage is turbulent and chaotic flow [21].

**Important note:**

The intensive mixing of the liquid in the turbulent flow promotes the transfer of heat between the mol ecules, which in turn increases the frictional force and convection heat.

### I-5-1-2 Dimensional Numbers for Forced Convection

#### 1-Nusselt number

The Nusselt number represents the enhancement of heat transfer through a fluid layer as a result of convection relative to conduction across the same fluid layer [18].

The larger nusselt number, the more effective convection [7].

$$Nu = \frac{hD}{k} = \frac{\dot{q}_{conv}}{\dot{q}_{cond}} \quad (I.13)$$

#### 2-Prandtl number

Is a measure of the relative thickness of the velocity and thermal boundary layer [7].

$$Pr = \frac{\text{molecular diffusivity of momentum}}{\text{molecular diffusivityof heat}} = \frac{\vartheta}{\alpha} = \frac{\mu C_P}{k} \quad (I.14)$$

Where :

$\vartheta$: Kinematic viscosity [$m^2/s$].

$\alpha = \frac{k}{\rho C_P}$ : Thermal diffusivity [$m^2/s$]. (I.15)

Cp: Specific heat capacity [J/kg.K].

k: Thermal conductivity [W/m· K].

μ: Dynamic viscosity [$N \cdot s/m^2$].

The prandlt number of gases is about 1, which indicates that both momentum and heat dissipate through the fluid at about the same rate.

Heat diffuses very quickly in liquid metals ($Pr \ll 1$) and very slowly in oils ($Pr \gg 1$) relative to momentum; hence, the thermal boundary layer is much thicker for liquid metals and much thinner for oils relative to the velocity boundary layer [22].

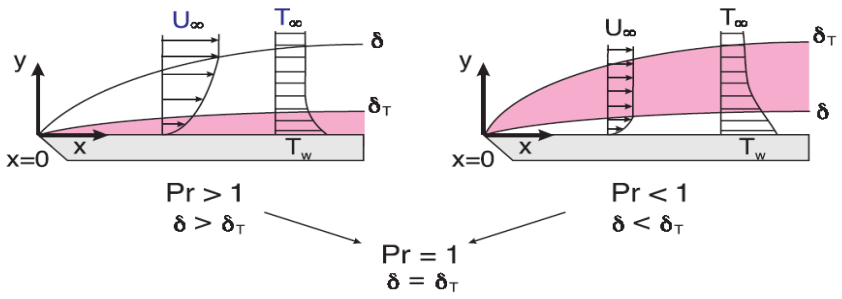


*Figure (I.10): The relation between the prandlt number and the thermal boundray layer and the velocity boundray layer [23].*

**3-Reynolds Number**

Is the ratio of inertial forces to viscous forces:

$$Re = \frac{\text{Inertial forces}}{\text{viscous forces}} = \frac{\rho v d}{\mu} \quad \text{(I.16)}$$

Used to categorize the fluid systems in which the effect of viscosity is important in controlling the flow pattern of a fluid, laminar or turbulent flow [7].

**Exemple :**

Re< 2000 A flow is considered laminar.

Re>3500 A flow is considered turbulent.

3500> Re >2000 is considered a transitional flow.

**I-5-1-3 Thermal Boundary Layer**

A thermal boundary layer develops when a fluid at a specified temperature flows over a surface that is at a different temperature.

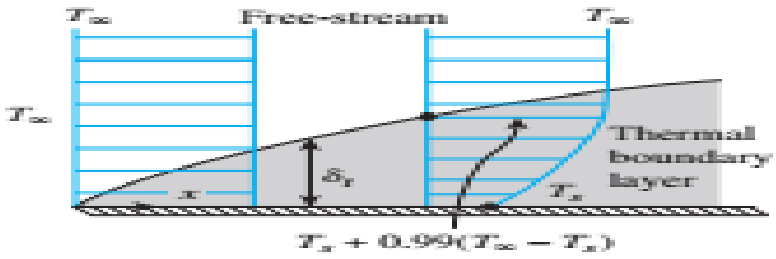


*Figure (I.11): Thermal boundray layer on a flat plate [24].*

The thickness of the thermal boundary layer $\delta_t$ at any location along the surface is defined as the distance from the surface at which the temperature difference $T-T_s$ equals 0.99 $(T_\infty-T_s)$

The thickness of the thermal boundary layer $\delta_t$ increases in the flow direction [22].

**I-5-2 Natural Convection**

In natural convection, fluid motion occurs by natural means such as buoyancy. where the fluid velocity is low, the heat transfer coefficient is low.

**Some examples are:** cooling of electronic equipment such as power transistors and TVS; heat transfer from electric baseboard heaters or steam radiator; heat transfer from refrigeration coils and power transmission lines; and heat transfer from the bodies of animals and human beings [25].

**Mechanisms of Natural Convection**

Consider a hot egg exposed to cold air. The temperature of the outside of the egg will drop (as a result of heat transfer with cold air), and the temperature of the adjacent air to the egg will rise. Consequently, the egg is surrounded by a thin layer of warmer air, and heat will be transferred from this layer to the outer layers of air.

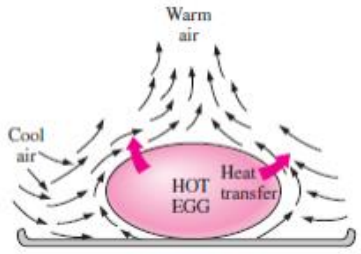


*Figure (I.12): Natural convenction heat transfer from a hot body (egg) [18].*

**Grashof number**

It is a dimentional number used to determine the dominance of natural convection over forced convection and is calculated by dividing the product of the buoyancy force and the characteristic length by the product of the viscous force and the thermal diffusivity. It helps in understanding the behavior of fluid flow and heat transfer in systems where natural convection plays a significant role [22]:

$$Gr = \frac{\text{buoyancy forces}}{\text{viscous forces}} = \frac{g\beta\Delta T\delta^3}{\vartheta^2} \quad (I.17)$$

We can also be represented as:

$$Gr = \frac{g\beta(T_s - T_\infty)\delta^3}{\vartheta^2} \quad (I.18)$$

g: Gravitaional acceleration $[m/s^2]$.

$\beta$: Coefficient of volume expansion [1 /K].

$\delta$: Characteristic lenghth of the geometry [m].

$\vartheta$: Kienmatics viscosity of the fluid $[m^2/s]$.

**Remarque :**

The Grashof number in natural convection played the same role as the Nusselt number in forced convection [26].

### I-5-3 Internel forced convection

The internal flow configuration is a practical geometry for energy conversion methods and the heating and cooling of fluids used in chemical processes. The flow is through pipes or ducts [18].

A fan or pump is typically used in these applications to compel the fluid to flow [22].

When considering the use of an internal flow, engineers should consider two fundamental considerations:

1-the heat transfer rate, or the thermal resistance between the stream and the walls.

2-The friction between the stream and the walls (the fluid friction is the same as the calculation of the pressure drop experienced by the stream over a finite length in the flow direction) [18].

**Note :**

Noncircular pipes (ducts) cannot bear severe deformation from huge pressure differentials between the inside and exterior, while circular pipes can.

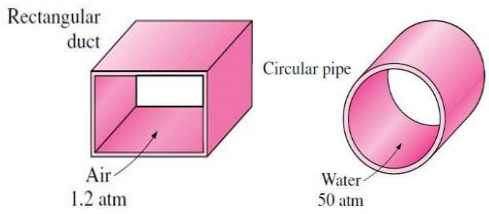


*Figure (I.13): The difference between the pressure in the circular pipes and ducts [27].*

### I-4-3-1 Average velocity and temperature

In the context of external flow, the free-stream velocity has been widely employed as a practical benchmark for determining the Reynolds number and the friction coefficient. However, in the case of internal flow, the absence of a free stream necessitates the adoption of an alternative approach. Within a tube, the fluid velocity experiences a transition from zero at the surface due to the no-slip condition to a maximum at the center of the tube. Consequently, it proves advantageous to utilize an average or mean velocity, denoted as $V_{avg}$, which remains constant in scenarios involving incompressible flow and a constant cross-sectional area of the tube.

The value of the average velocity $V_{avg}$ at some streamwise cross section is determined by the requirement that the conservation of mass principle be satisfied, which is [27]:

$$\dot{m} = \rho V_{avg} A_c = \int_{A_c} \rho u(r) dA_c \qquad (I.19)$$

$\dot{m}$: The mass flow rate.

$\rho$: The density.

$A_c$: The cross-sectional area.

u (r):The velocity profile.

The expression for the average velocity of incompressible flow in a circular pipe with a radius of R can be written as :

$$V_{avg} = \frac{\int_{A_c} \rho u(r) dA_c}{\rho A_c} = \frac{\int_0^R \rho u(r) 2\pi r dr}{\rho \pi R^2} = \frac{2}{R^2}\int_0^R u(r) r dr \quad (I.20)$$

The value of the mean temperature $T_m$is determined by ensuring that the conservation of energy principle is satisfied. Unlike the mean velocity, the mean temperature $T_m$ changes in the direction of flow whenever the fluid is heated or cooled. To simplify calculations in fluid flow analysis, it is convenient to work with an average or mean temperature $T_m$, which remains constant at each cross section [27].

This can be expressed mathematically as:

$$\dot{E}_{fluid} = \dot{m} C_p T_m = \int_{\dot{m}} C_p T(r) \delta\dot{m} = \int_{A_c} \rho C_p T(r) u(r) dA_c \quad (I.21)$$

$C_p$: specific heat of the fluid.

Then, the mean temperature of a fluid with constant density and specific heat flowing in a circular pipe of radius R can be expressed as [27]:

$$T_m = \frac{\int_{\dot{m}} C_p T(r) \delta\dot{m}}{\dot{m} C_p} = \frac{\int_0^R C_p T(r) \rho u(r) 2\pi r dr}{\rho V_{avg} (\pi R^2) C_p} = \frac{2}{V_{avg} R^2}\int_0^R T(r) u(r) dr \quad (I.22)$$

**I-4-3-2 The Entrance region and Fully developed region**

Fluid enters a circular tube at a uniform speed, due to the no-slip condition, The tube's flow is divided into two sections: the boundary layer region, which has substantial viscous effects and velocity changes, and the inviscid (core) flow zone, which has negligible frictional effects and constant radial velocity [27].

The thickness of this boundary layer increases in the flow direction until the boundary layer reaches the center of the tube, thus filling the entire tube, where the velocity becomes fully developed slightly downstream [28].

The region from the pipe inlet to the point at which the velocity profile is fully developed is called the hydrodynamic entrance region, and the length of this region is called the hydrodynamic entry length $L_h$ [15].

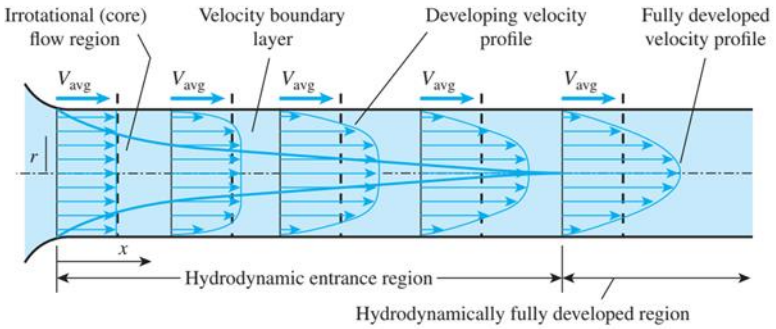


*Figure (I.14): The development of the velocity boundary layer in a pipe [22].*

- Entrance region ( hydrodynamically developing region): $u = u(r, x)$ [22].
- Hydrodynamically fully developed : $\frac{\partial u(r,x)}{\partial x}=0 \Rightarrow u=u(r)$ [27] .

The region where the thermal boundary layer develops and reaches the center of the tube is called the thermal entrance region, and the length of this region is called the thermal entry length ($L_t$). Flow in the thermal entrance region is called thermally developing flow.

The region where the dimensionless temperature profile remains unchanged is called the thermally fully developed region, expressed by the dimensionless temperature profile, and it is represented by the dimensionless temperature profile. $(T_s - T)/(T_s - T_m)$ [27].

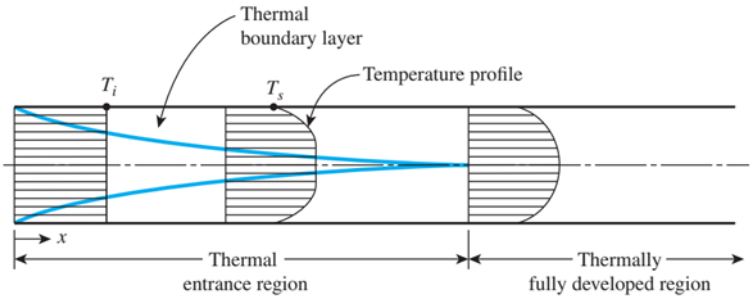


*Figure (I.15): The development of the thermal boundary layer in a tube [22].*

Thermally fully developed :

$$\frac{\partial}{\partial r}\left(\frac{T_s - T}{T_s - T_m}\right)_{r=R} = \frac{-(\partial T/\partial r)_{r=R}}{T_s - T_m} \neq f(x) \quad \text{(I.23)}$$

**Entry Lengths**

In laminar flow, the hydrodynamic and thermal entry lengths are given approximately as [see Kays and Crawford (1993) and Shah and Bhatti (1987)].

$$L_{h,lam} \approx 0.05 Re_D D_h \quad \text{(I.24)}$$

$$L_{t,lami} \approx 0.05 Re_D Pr.\, D = Pr L_{h,Lami} \quad \text{(I.25)}$$

The entry length is much shorter in turbulent flow, where the hydrodynamic and thermal entry lengths are approximately given [18].

$$L_{h,turbulent} \approx L_{t,turbulent} \approx 10D \quad (I.26)$$

**Note :**

If Pr > 1, the hydrodynamic boundary layer develops more rapidly than the thermal boundary layer.

For turbulent flow, conditions are nearly independent of the Prandtl number [18].

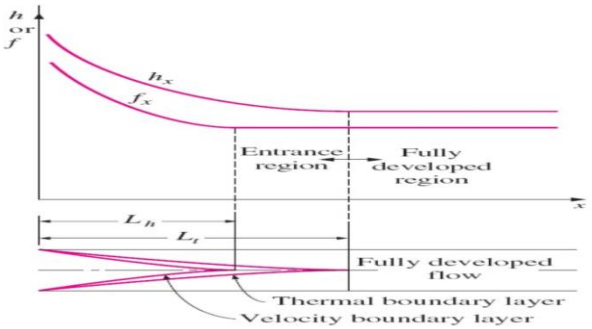


*Figure (I.16): Variation of the friction factor and the convection heat transfer heat transfer cofficient in the flow direction for flow in a tube (Pr<1) [18].*

### I-4-3-3 General thermal analysis

In the absence of any work interactions (such as electric resistance heating), the conservation of energy equation for the steady flow of a fluid in a tube can be expressed as [27]:

$$\dot{Q} = \dot{m}C_p(T_e - T_i) \quad (I.27)$$

Where :

$T_i$: Mean fluid temperature at the tube inlet.

$T_e$: Mean fluid temperature at the tube exit.

$C_p$: Specific heat capacity.

$\dot{m}$: Mass flow rate.

Surface heat flux is expressed as:

$$\dot{q}_s = h_x (T_s - T_m) \quad (I.28)$$

Where:

$\dot{q}_s$: Constant surface heat flux .

$h_x$: The local heat transfer coefficent .

$T_s$: The constant surface fluid temperature.

$T_m$: The mean fluid temperature.

**Constant surface heat flux ($\dot{q}_s = constant$):**

The rate of heat transfer it's expressed as:

$$\dot{Q} = \dot{q}_s \times A_s = \dot{m} C_p (T_e - T_i) \quad (I.29)$$

Mean fluid temperature at the tube exit [22]:

$$T_e = T_i + \frac{\dot{q}_s \times A_s}{\dot{m} C_p} \quad (I.30)$$

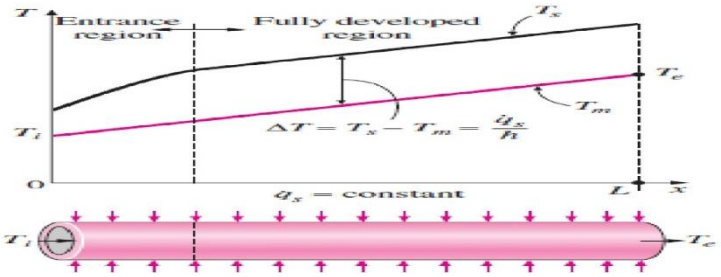


*Figure (I.17): Variation of the tube surface and the mean fluid temperatures along the tube [27].*

**steady flow energy balance :**

$$\dot{m} C_p dT_m = \dot{q}_s (p dx) \quad (I.31)$$

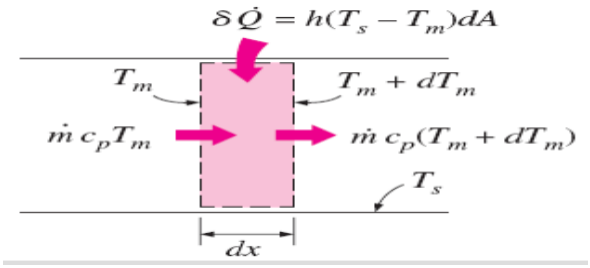


*Figure (I.18): Energy interactions for a differential control volume in a tube [27].*

**Constant Surface Temperature (Ts = constant):**

The rate of heat transfer to or from a fluid flowing in tube:

$$\dot{Q} = h A_s \Delta T_{ave} = h A_s (T_s - T_m)_{ave} \quad (I.32)$$

We have two suitable ways to express $\Delta T_{ave}$:

**1**-Arithmetic mean temperature difference:

$$\Delta T_{ave} \approx \Delta T_{am} = \frac{\Delta T_i + \Delta T_e}{2} = \frac{(T_s - T_i) + (T_s - T_e)}{2} = T_s - \frac{T_i + T_e}{2} = T_s - T_b \quad (I.33)$$

$T_b$ it's the bulk mean temperature where:

$$T_b = \frac{Ti+Te}{2} \quad (I.34)$$

By using the arithmetic mean of the temperature differences, we assume that the mean fluid temperature changes linearly along the pipe, which is rare if $T_s$= constant.

This simple approximation usually produces acceptable results, but not always, so we need a better way to evaluate $dT_{ave}$ [27].

**2**-The energy balance on a differential control volume gives:

$$\dot{m}C_p dT_m = h(T_s - T_m)dA_s \quad (I.35)$$

The above relation can be rearranged as follows :

$$\frac{d(T_s-T_m)}{T_s-T_m} = -\frac{hp}{\dot{m}C_p}dx \quad (I.36)$$

By using the integration from x=0 (tube inlet $T_m$=$T_i$) to x=L (tube exit $T_m$=$T_e$) we found [18]:

$$\ln\frac{T_s-T_e}{T_s-T_i} = -\frac{hA_s}{\dot{m}C_p} \quad (I.37)$$

The mean fluid temperature in the exit of tube is:

$$T_e = T_s - (T_s - T_i)e^{\frac{-hA_s}{\dot{m}Cp}} \quad (I.38)$$

After we can represent the log mean temperature like [29]:

$$\dot{Q} = hA_s\Delta T\ln \quad (I.39)$$

$$\Delta T_{lm} = \frac{T_i-T_e}{\ln\left[\frac{T_s-T_e}{T_s-T_i}\right]} = \frac{\Delta T_e-\Delta T_i}{\ln\left[\frac{\Delta T_e}{\Delta T_i}\right]} \quad (I.40)$$

**where:**

$\Delta T_{lm}$: The log mean temperature difference.

### I-4-3-4 Laminar flow in tubes

As we discussed earlier, the flow is laminar when the Reynolds number is less than or equal to 2300. Under such conditions, the fluid's viscous forces are dominant, leading to a highly organized flow of the fluid layers.

The Nusselt number is critical for predicting the effectiveness of heat transfer between the fluid and the surface of the tube. Therefore, we will explore some of the various Nusselt number values established by scientists for different cases [30].

This value can be a critical baseline for engineers and scientists to design systems involving heat exchangers, medical devices, and other applications where precise thermal management is essential.

Constant Surface Heat Flux ( $\dot{q}_s = \text{constant}$ ) (Circular Tube,Laminar):

$$Nu = \frac{hD}{k} = 4.36 \quad \text{(I.41)}$$

Constant Surface Temperature ($T_s = \text{constant}$):

$$Nu = \frac{hD}{k} = 3.66 \quad \text{(I.42)}$$

**Developing Laminar Flow in the Entrance Region**

The average Nusselt number for the thermal entrance region can be determined from [Edwards et al., 1979] [22]:

$$Nu = 3.66 + \frac{0.065(D/L)Re\ Pr}{1+0.04[(D/L)RePr]^{2/3}} \quad \text{(I.43)}$$

The average Nusselt number for hydrodynamically and thermally developing laminar flow in a circular tube in that case can be determined from [Sieder and Tate (1936)] [22]:

$$Nu = 1.86\left(\frac{RePrD}{L}\right)^{1/3}\left(\frac{\mu_b}{\mu_s}\right)^{0.14} \quad \text{(I.44)}$$

The average Nusselt number for the thermal entrance region of flow between isothermal parallel plates of length L is expressed as (Edwards et al., 1979) [22]:

$$Nu = 7.54 + \frac{0.03(D_h/L)RePr}{1+0.016[(D_h/L)RePr]^{2/3}} \quad \text{(I.45)}$$

## Laminar Flow in Noncircular Tubes

*Table (I.1): Nusselt number and friction factor for fully developed laminar flow in tubes of various cross sections [18].*

| Tube Geometry | a/b or θ° | Nusselt Number $T_s$ = Const. | Nusselt Number $\dot{q}_s$ = Const. | Friction Factor f |
|---|---|---|---|---|
| Circle 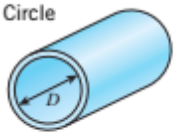 | — | 3.66 | 4.36 | 64.00/Re |
| Rectangle 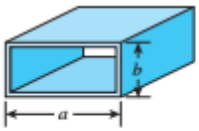 | a/b | | | |
| | 1 | 2.98 | 3.61 | 56.92/Re |
| | 2 | 3.39 | 4.12 | 62.20/Re |
| | 3 | 3.96 | 4.79 | 68.36/Re |
| | 4 | 4.44 | 5.33 | 72.92/Re |
| | 6 | 5.14 | 6.05 | 78.80/Re |
| | 8 | 5.60 | 6.49 | 82.32/Re |
| | ∞ | 7.54 | 8.24 | 96.00/Re |
| Ellipse 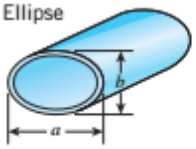 | a/b | | | |
| | 1 | 3.66 | 4.36 | 64.00/Re |
| | 2 | 3.74 | 4.56 | 67.28/Re |
| | 4 | 3.79 | 4.88 | 72.96/Re |
| | 8 | 3.72 | 5.09 | 76.60/Re |
| | 16 | 3.65 | 5.18 | 78.16/Re |
| Isosceles Triangle 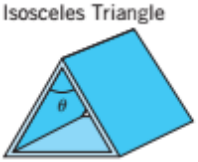 | θ | | | |
| | 10° | 1.61 | 2.45 | 50.80/Re |
| | 30° | 2.26 | 2.91 | 52.28/Re |
| | 60° | 2.47 | 3.11 | 53.32/Re |
| | 90° | 2.34 | 2.98 | 52.60/Re |
| | 120° | 2.00 | 2.68 | 50.96/Re |

### I-4-3-5 Turbulent flow in tubes

Earlier, it was stated that flow in smooth tubes typically becomes fully turbulent when the Reynolds number exceeds 10,000. Turbulent flow is frequently preferred in practical applications due to the higher heat transfer coefficients it offers. Empirical studies are often relied upon to establish correlations for friction and heat transfer coefficients in turbulent flow, as theoretical analysis of turbulent flow poses significant challenges. In the case of smooth tubes, the friction factor in turbulent flow can be calculated [27].

**First Petukhov equation [Petukhov (1970)] given as:**

For smooth tubes:

$$f = (0.790 \ln R_e - 1.64)^{-2} \qquad 3000 < R_e < 5\times 10^6 \tag{I.46}$$

- **The Chilton–Colburn analogy:**

The relationship between the Nusselt number in turbulent flow and the friction factor can be described by the Chilton–Colburn analogy, which is expressed as [27]:

$$N_u = 0.125 f R_e P_r^{\frac{1}{3}} \tag{I.47}$$

❖ **The Colburn equation is known as:**

$$N_u = 0.023 R_e^{0.8} P_r^n \qquad (0.7 \leq P_r \leq 160) \text{ and } (R_e > 10{,}000) \qquad \text{(I.48)}$$

Where :

n=0.3 for cooling.

n=0.4 for heating .

❖ **The equation of Sieder and Tate (1936) is:**

$$N_u = 0.027 R_e^{0.8} P_r^{\frac{1}{3}} \left(\frac{\mu_b}{\mu_s}\right)^{0.14} \qquad (0.7 \leq P_r \leq 16{,}700) \text{ and } (R_e > 10{,}000) \qquad \text{(I.49)}$$

❖ **The secnond Petukhov equation:**

The Nusselt number relations that we saw before are simple, but they may give errors as much as 25%. This error can be reduced to less than 10 % by using more complex and accurate relations, such as the second Petukhov equation defined as [27]:

$$Nu = \frac{\left(\frac{f}{8}\right).Re.Pr}{1.07+12.7\left(\frac{f}{8}\right)^{0.5}.\left(Pr^{\frac{2}{3}}-1\right)} \qquad (10^4 < Re < 5.10^6) \text{ and } \quad (0.5 \leq Pr \leq 2000) \qquad \text{(I.50)}$$

❖ **This relation is improved by modifying it as Gnielinski (1976):**

$$Nu = \frac{\left(\frac{f}{8}\right).(Re-1000).Pr}{1+12.7\left(\frac{f}{8}\right)^{0.5}.\left(Pr^{\frac{2}{3}}-1\right)} \qquad (0.5 \leq Pr \leq 2000) \quad \text{and} \quad (3.10^3 < Re < 5.10^6) \qquad \text{(I.51)}$$

❖ **Sleicher and Rouse (1975) as:**

For liquid metals (0.004 < Pr <0.01), the following relations are recommended by Sleicher and Rouse (1975) as:

$$Ts = \text{constant} \qquad Nu = 4.8 + 0.0156 Re^{0.85}.Pr^{0.93} \qquad \text{(I.52)}$$

$$\dot{q}_S = \text{constant} \qquad Nu = 6.3 + 0.0167 Re^{0.85}.Pr^{0.93} \qquad \text{(I.53)}$$

**I -6- Heat Transfer Enhancement**

Enhancing heat transmission has always been a very intriguing issue in the quest to create tiny, lightweight, inexpensive, and highly efficient heat exchangers. Researchers are also motivated to outperform the current designs by the cost of energy and environmental concerns [31].

During the last century, many studies have been conducted to better control wall heat transfer and reduce the boundary layers. These studies have been increasing since the early 1960s. Mainly, the classification is based on the mode of contact with the fluid and the surface, and we can classify them into two categories: passive and active [31].

### I-6-1 Important Terminologies

#### I-6-1-1 Thermal Enhancement Factor

This term η is used for characterizing the thermal enhancement capacity of a tube, which is given as:

$$\eta = (Nu/Nu_o)/(f/f_o) \quad (I.54)$$

Where the subscript 'o' is for the plain tube.

**Note :**

Should be η >1, but if it is not This means that the tube surface is not effective in enhancing heat and pumping power is consumed in increasing the pressure to overcome the frictional loss [32].

#### I -6-1-2 Entropy generation rate

$\dot{S}_{gen}$ is the rate of entropy generation,This is given as [32]:

$$\dot{S}_{gen} = \sum \left(\frac{\dot{Q}}{T}\right)_{out} - \sum \left(\frac{\dot{Q}}{T}\right)_{in} + \frac{\dot{Q}_{irr}}{T_{avg}} \quad (I.55)$$

Where :

$\dot{Q}_{irr}$ : Internal entropy.

$T_{avg}$ : Average temperature.

### I-6-2 Active Methods

Active techniques are more complex than passive techniques in the expression of design and application because they involve the use of some external power or resource to generate heating [33].

And they are also used as an active means to enhance heat transfer through vibration of the surface or fluid. The electrostatic field, jet impingement (used for heat and cooling as well; example: cooling of gas turbine blades), and the use of active techniques in scientific fields are limited [32].

### I-6-3 Passive Methods

The passive method involves direct heat transfer by modification of the hardware, in the sense of modifying the heat exchange surface area and the physical properties of the surface or liquid to increase the thermohydraulic performance of the systems [34].

The inserts, ribs, and rough surfaces are utilized to promote fluid mixing and turbulence in the flow, which results in an increase in the overall heat transfer rate [33].

Increasing the effective surface area and residence time of the heat transfer fluids is an illustration of one of these techniques. This method improves effective surface area, residence duration, and the

heat transfer coefficient in an existing system by causing the bulk of the fluids to swirl and disturbing the real boundary layers [35].

### I-6-3-1 Rough surfaces

They are generally surface modifications that promote turbulence in the flow field, primarily in single-phase flows, and do not increase the heat transfer surface area. Their geometric features range from random sand-grain roughness to discrete three-dimensional surface protuberances [35].

The thermal performance of the systems improves significantly compared to that of a smooth surface [36].

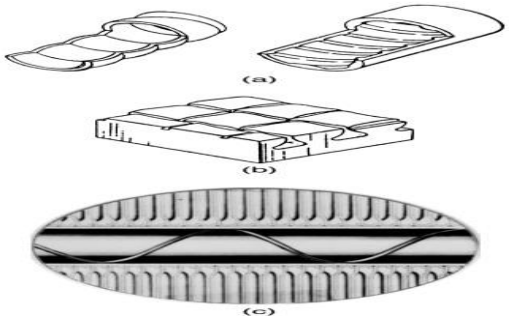


*Figure (I.19) :Tube-side roughness for single-phase flow;(b) rough surface for nucleate boiling; (c) wire-coil insert which periodically distrubs the boundary layer [37].*

An example of a study by Soon-Tarapironsook in 2020 on the application of a plate heat exchanger with a grooved surface noted that performance could be improved by 20.102% to 46.12% by increasing surface roughness [36].

### I-6-3-2 Extended surfaces

They effectively increase heat transmission. The most recent advances have resulted in redesigned fin surfaces that, in addition to increasing surface area, also tend to increase heat transfer coefficients by disrupting the flow field [35].

An example of this is a study by Borhani et al. in 2019 on the application of a heat exchanger with helical fins for wate, we remarque that the spiral-fin improves the heat transfer rate by about 56 % [36].

### I-6-3-3 Swirl flow

They create secondary recirculation or swirl flow, which they then superimpose over the axial flow of a channel. Twisted tapes and helical strip or cored screw-type tube inserts are examples of these devices. They are applicable to both single-phase and two-phase flows heat-exchangers [35].

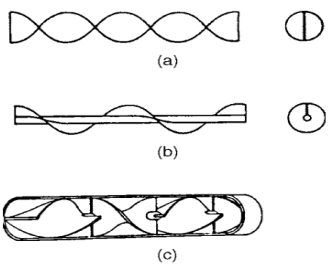


*Figure (I.20): Three types of swirl flow inserts :(a) twisted -tape insert ,(b) helical vane insert ,(c) static mixer [37].*

### I-6-3-4 Coiled tubes

These methods work well with heat exchangers that are comparatively smaller in size. The secondary flows and vortices created by coiled tubes increase the heat transfer coefficient in single-phase flow and most boiling regions [35].

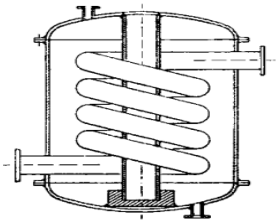

*Figure (I.191): Helically coiled tube heat exchange [37].*

### I-6-3-5 Surface tension

These consist of wicking or grooved surfaces, which direct and improve the flow of liquid to boiling surfaces and from condensing surfaces [38].

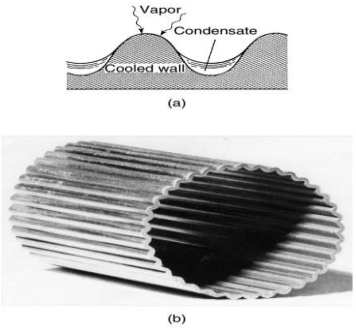


*Figure (I.22): (a) Illustration of surface tension drainage from the flutes into drainage channels (b) Fluted tube used for condensation in the vertical orientation [37].*

### I-6-3-6 Additives for liquids

These include the addition of solid particles, soluble trace additives, and gas bubbles into single-phase flows and trace additives, which usually depress the surface tension of the liquid for boiling systems [35].

### I-6-3-7 Additives for Gases

These include liquid droplets or solid particles, which are introduced in single-phase gas flows either as dilute phases (gas-solid suspensions) or as dense phases (fluidized beds) [38].

### I-6-4 Insert

In past years, inserts such as twisted tapes, winglets, swirl generators, baffles, etc. have been considered one of the most effective passive heat transfer techniques for different systems [36].

### I-6-4-1 Twisted Tape

In order to increase heat transmission, twisted tapes are made of metallic strips that have been twisted in a variety of ways to give them the right form and dimension before being introduced into the flow. Twisted tape inserts are perfect for this and are frequently used in heat exchangers [39].

### I-6-4-2 Baffles

Flow-directing panels, or baffles, are used to control the flow of liquid or gas. Because dead zones are eliminated, pressure drop is decreased when helical baffles are used. Heat transmission therefore improves even if these regions are reduced [36].

### I-6-4-3 Winglets

The rotating flow that results when winglets are present provides sufficient temperature dispersion in both the linear and radial directions.

A better temperature distribution is produced in the models than in the conventional geometry due to the existence of obstacles in the flow direction and the turbulence that results from them. One thing to note about the use of winglets is the fluid employed, which is air fluid in the majority of the studied publications [36].

The figure shows the streamlines of the flow to help visualize how the winglet affects the flow structure and heat transfer enhancement mechanisms of the systems. A counter-spinning vortex is produced by the winglets and appears along the duct, whereas a flat plate shows the absence of a vortex. A notable increase in heat exchange is caused by this phenomenon.

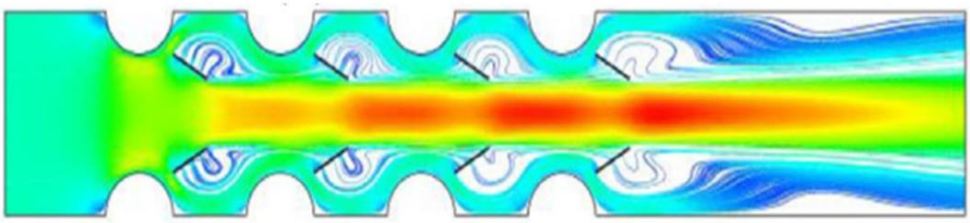

*Figure (I.23): The streamline with the contour of velocity [36].*

**I-7 vortex generators**

Vortex generators are efficient aerodynamic devices that are widely utilized in both external and internal aerodynamics to control the flow. These devices create local geometric imperfections, resulting in the formation of linear vortices. These vortices promote mixing of the flow, energize the boundary layer, and effectively delay or prevent separation.

Additionally, they induce secondary flow motion, which alters the overall flow pattern. The specific geometrical characteristics of vortex generators depend heavily on the flow propreties and the nature of the problem at hand.

Therefore, it is advantageous to employ advanced computational-fluid-dynamics (CFD) techniques in conjunction with experimental data and statistical methods to optimize their design and performance [40].

The vortex generator geometry (Figure I. 20) utilized to produce pairs of counter-rotating vortexes in close proximity to the wall is outlined in Table (I.6).

The blade angle is set at 15 degrees, adhering to the circuitry proposed by Pearcy in 1961.

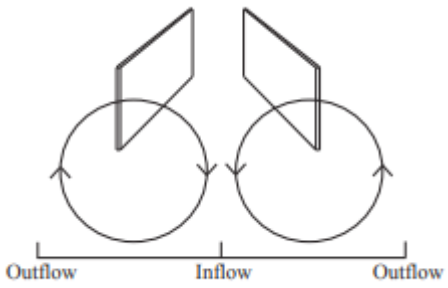


*Figure (I.21) :Vortex generators geometry [41].*

For a VG pair where U is the mean velocity at the VG blade tip with a constant blade angle for all configurations, we have :

$$\Gamma e = 2hU \tag{I.56}$$

In the case of the VG pair, it is important to note that the estimated production of circulation increases in a linear fashion as the blade height (h) increases [41].

However, for the array the VG density increases as the blade height decreases, specifically when the ratio of (h) to D remains constant .This parameter makes $\gamma_e$:

$$\gamma_e = 2\frac{hU}{D} \tag{I.57}$$

### I-7-1 Use of vortex generators to improve heat transfer in heat exchange

The utilization of vortex generators represents a promising strategy to enhance heat transfer in various heat exchange systems. Vortex generators are devices designed to induce controlled swirling flows, or vortices, in the fluid, thereby promoting better mixing and increasing heat transfer rates. These devices come in various shapes and configurations, such as fins, ribs, or delta wings, strategically placed within the flow path. By introducing vortices into the fluid flow, vortex generators disrupt the boundary layer and reduce the thickness of the thermal boundary layer, facilitating more efficient heat transfer between the fluid and the heat exchange surface. This enhanced heat transfer capability can lead to improvements in the overall performance and efficiency of heat exchangers across a range of applications, including air conditioning systems, refrigeration units, and thermal power plants. Moreover, the design and optimization of vortex generators offer a versatile and cost-effective means to achieve higher heat transfer rates while minimizing energy consumption, making them a valuable tool in the quest for more sustainable and efficient heat exchange technologies [42].

### I-8 Heat exchange in solar concentrator absorbers

Heat exchange in solar concentrator absorbers is a critical process that facilitates the efficient conversion of solar energy into usable heat. Solar concentrator absorbers, typically composed of materials with high thermal conductivity, such as metals or ceramics, absorb sunlight and transfer the generated heat to a working fluid or storage medium. This heat exchange is essential for applications ranging from solar water heating systems to concentrated solar power plants. By maximizing the contact between the absorber material and the incoming solar radiation, along with optimizing the heat transfer mechanisms, solar concentrator absorbers can achieve high thermal efficiencies, making them indispensable components in solar energy systems [43].

### I-9 Conclusion

In conclusion, a variety of engineering applications require a grasp of fluid classification and convection principles. Both induced and spontaneous convection are important for heat transfer systems. In engineering systems, forced convection occurs often in two situations: internally within tubes and externally across surfaces. The behavior of heat transfer is greatly influenced by variables such as average velocity, temperature distribution, and flow regimes including laminar and turbulent flows. Furthermore, optimizing thermal systems depends on improving heat transport using passive techniques like vortex generators and active techniques like inserts. Through a thorough understanding of these subjects, engineers can create more effective and efficient heat transfer systems, advancing both industry and technology.

# CHAPTER II
# MATHEMATICAL FORMULATION AND NUMERICAL MODELING

## II-1 Introduction

Thermal exchanges play a crucial role in various sectors of human activities. The objective of this study is to solve heat transfer problems with flow using a computational code called "Fluent," which is based on the numerical method of finite volumes. The geometry, meshing, and boundary conditions are determined using a preprocessor named "Gambit," while the simulation parameters are set at the "Fluent," processor level. Based on our obtained results, it has been observed that in order to achieve accurate results, it is necessary to choose a mesh that is suitable for the studied configuration. The distribution of velocity, temperature, and pressure exhibits good agreement with reality. A comparison is made between the results obtained from Fluent and those obtained from empirical relations and experiments to determine the distribution of the Reynolds number and the Nusselt number. This comparison leads to the conclusion that Fluent is an excellent choice for accurately simulating these heat transfer problems, as we have found very close and sometimes overlapping curves.

## II-2 Gouvernant equation

We study moving fluids by developing basic equations in an integrated form to be applied to the control of volumes (i.e., a stationary area). One of the reasons for choosing volume control over a system (i.e., mass) is our interest in the effect of fluid movement on devices (e.g., a tubular elbow) rather than the movement of a certain mass of fluid [8].

We therefore apply the Reynolds transport theorem (the rate of change of the property of an arbitrary total fluid) to mass, linear momentum, angular momentum, and energy in the sense of deriving the four basic control volume relations of fluid mechanics [44].

$$\frac{dB_{sys}}{dt} = \frac{d}{dt}\int_{CV}\rho b d\mathcal{V} + \int_{CS}\rho b(\vec{V}.\vec{n})dA \qquad (II.1)$$

### II-2-1 Conservation of Mass

A system is a random collection of substances with a fixed identity; it consists of the same amount of substance at all times. The conservation of mass requires that the mass of the system be constant based on the rate [8].

$$m_{sys} = const \Longrightarrow \frac{dm_{sys}}{dt} = 0 \qquad (II.2)$$

**Preservation of the principle of mass :**

The principle of conservation of mass for the control volume can be expressed as follows [45]:

$$\begin{pmatrix}\text{Total mass entering}\\ \text{the CV during}\Delta t\end{pmatrix} - \begin{pmatrix}\text{Total mass leaving}\\ \text{the CV during }\Delta t\end{pmatrix} = \begin{pmatrix}\text{within the CV during}\\ \text{Net change in mass }\Delta t\end{pmatrix}$$

$$m_{in} - m_{out} = \Delta m_{CV} \qquad (II.3)$$

The conservation of mass principle for a general steady-flow system with multiple inlets and outlets can be expressed in rate form as :

$$\dot{m}_{in} - \dot{m}_{out} = \frac{dm_{cv}}{dt} \qquad (II.4)$$

$$\sum_{in}\dot{m} = \sum_{out}\dot{m} \qquad (II.5)$$

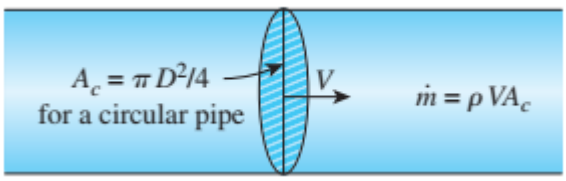


*Figure(II.1): The mass flow rate at a cross section to the product of the fluid density [45].*

.

**General conservation of mass:**

Compensation in Reynolds transport theory (B=m, b=m/m=1)

$$\frac{d}{dt}\int_{CV}\rho d\mathcal{V} + \int_{CS}\rho(\vec{V}.\vec{n})dA = 0 \quad \text{(II.6)}$$

If the flow is steady( $\rho = \text{constant}$) then:

$$\partial\rho/\partial t = 0 \quad \text{(II.7)}$$

The equation:

$$\int_{CV}\rho V dA = 0 \quad \text{(II.8)}$$

**Mass and Volume Flow Rates:**

The mass flow rate , is defined by:

$$\dot{m} = \int_{A}\rho V dA \quad \text{(II.9)}$$

The volume flow rate, is defined by:

$$\dot{V} = \int \rho V dA_C \quad \text{(II.10)}$$

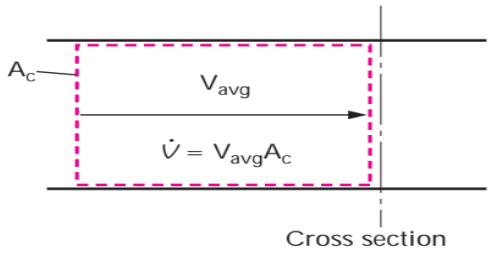


*Figure(II.2): The volume flow rate is the volume of fluid flowing through a cross section per unit time[45].*

**Special Case:**

**Incompressible Flow**

Steady, incompressible flow:

Where: $\rho = \text{constant}$

$$\sum_{in}\dot{V} = \sum_{out}\dot{V} \Rightarrow \sum_{in}A_1V_1 = \sum_{out}A_2V_2 \quad \text{(II.11)}$$

Steady, incompressible flow (single stream): $\dot{V}_1 = \dot{V}_2 \Rightarrow A_1V_1 = A_2V_2$

The equation of conservation of mass for a steady flow,tow dimensional:

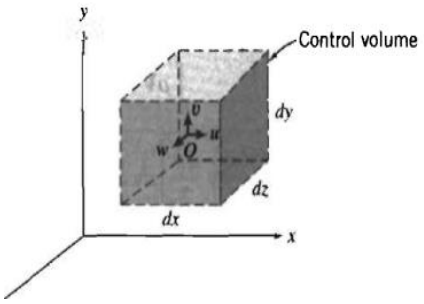


*Figure(II.3): Differential control volume in rectongular Coordinates.*

A mass flux through the control surface of a rectangular differential control volume ($\int_{CV}\rho\vec{V}d\vec{A}$) [8].

Following(+x): $\left[\rho+\left(\frac{\partial\rho}{\partial x}\right)\frac{dx}{2}\right]\left[u+\left(\frac{\partial u}{\partial x}\right)\frac{dx}{2}\right]dy=\rho udy+\frac{1}{2}\left[u\left(\frac{\partial\rho}{\partial x}\right)+\rho\left(\frac{\partial u}{\partial x}\right)\right]dxdy$ (II.12)

Following (+y): $\left[\rho+\left(\frac{\partial\rho}{\partial y}\right)\frac{dy}{2}\right]\left[u+\left(\frac{\partial v}{\partial y}\right)\frac{dy}{2}\right]dx=\rho vdx+\frac{1}{2}\left[v\left(\frac{\partial\rho}{\partial y}\right)+\rho\left(\frac{\partial v}{\partial y}\right)\right]dxdy$ (II .13)

Then:

$$\int_{Cs}\rho\vec{V}d\vec{A}=\left[\left(\frac{\partial\rho u}{\partial x}\right)+\left(\frac{\partial\rho v}{\partial y}\right)\right]dxdy \quad (II.14)$$

for a steady ,tow dimensional the differential equation for conservation of mass is then:

$$\left(\frac{\partial\rho u}{\partial x}\right)+\left(\frac{\partial\rho v}{\partial y}\right)+\left(\frac{\partial\rho}{\partial t}\right)=0 \quad (II.15)$$

**II-2-2 Conservation of Energy**

The conservation of energy principle, also known as the **first law of thermodynamics,** states that energy can neither be created nor destroyed during a process; it can only change forms for every system going through any process. the conservation of energy (energy balance) concept may be stated as follows:

$$\begin{pmatrix}\text{Total energy}\\ \text{entering the}\\ \text{system}\end{pmatrix}-\begin{pmatrix}\text{Total energy}\\ \text{leaving the}\\ \text{system}\end{pmatrix}=\begin{pmatrix}\text{Change in the}\\ \text{total energy of}\\ \text{the system}\end{pmatrix}$$

$$E_{in}-E_{out}=\Delta E_{system} \quad (II.16)$$

Noting that energy can be transferred to or from a system by heat, work, and mass flow and that the total energy of a simple compressible system consists of internal kinetic, and potential energies [46].

In the **rate form** as:

$$\dot{E}_{in}-\dot{E}_{out}=\Delta E_{system}/dt \quad (II.17)$$

If the state of the system does not change during a process, the energy of the system is zero ($\Delta E_{system}=0$) that is, the process is constant.

**Steady rate form**

$$\dot{E}_{in} = \dot{E}_{out} \quad \text{(II.18)}$$

The total energy of a system during a process is the change in its internal energy (in the absence of significant electric, magnetic, motion, gravity, and surface tension effects).

$$\Delta E_{system} = \Delta U_{system} \quad \text{(II.19)}$$

**Stationary closed system**

It is a system that does not allow the exchange of matter with the outside medium, and the mass of matter in this system is constant (such as a covered watter bottle), so there are no changes in its speed or height during the process [46].

$$E_{in} - E_{out} = \Delta U = mc_V \Delta T \quad \text{(II.20)}$$

Where:

$\Delta T$: The temperature change.

$c_V$: The specific heat at constant volume.

For a closed system, the following relation between work and heat based on the first law can be written:

$$\Delta E = Q - W \quad \text{(II.21)}$$

Stationary closed system no work:

$$Q = mc_V \Delta T \quad \text{(II.22)}$$

The rate of net heat transfer into or out of the control volume. This is the form of the energy balance relationship that we will use most often for steady-flow systems.

$$\dot{Q} = \dot{m}\Delta h = \dot{m}c_p \Delta T \ [Kj/s] \quad \text{(II.23)}$$

**Surface Energy Balance**

$$\dot{E}_{in} = \dot{E}_{out} \quad \text{(II. 24)}$$

**Example:**

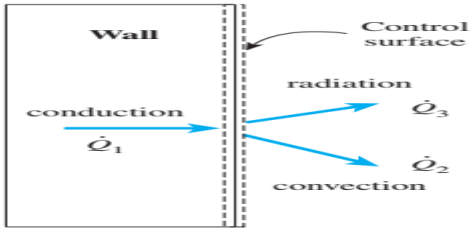


*Figure(II. 4): Surface energy balance [45].*

**General conservation of energy**

Compensation in Reynolds transport theory (B=E,b=e)

$$\frac{dE_{sys}}{dt} = \frac{d}{dt}\int_{CV} e\rho d\mathcal{V} + \int_{CS} e\rho(\vec{V}.\vec{n})A \quad (II.25)$$

The enargy equation is obtained by applying the principle of the conservation of the energy in the (x) and (y) direction as follows [47]:

$$u\frac{\partial T}{\partial x} + v\frac{\partial T}{\partial y} = \alpha\left(\frac{\partial^2 T}{\partial x^2} + \frac{\partial^2 T}{\partial y^2}\right) \quad (II.26)$$

## II-2-3 Conservation of mouvement

When the system of masses is completely isolated from all forms of external force or when the sum of external forces is equal to zero at all times, there is conservation of motion in time for the entire system.

For a rigid body of mass m, Newton's second law is expressed as:

$$\vec{F} = m\vec{a} = m\frac{d\vec{V}}{dt} = \frac{d(m\vec{V})}{dt} \quad (II.27)$$

**The forces acting on a control volume**

The forces acting on a control volume consist of body forces that act throughout the entire body of the control volume (such as gravity, electric, and magnetic forces) and surface forces that act on the control surface (such as pressure and viscous forces and reaction forces at points of contact) [45].

Total force acting on the control volume:

$$\sum \vec{F} = \sum \vec{F}_{body} + \sum \vec{F}_{surface} \quad (II.28)$$

The differential body force $d\vec{F}_{body} = d\vec{F}_{gravity}$ acting on the small fluid element:

Gravitational force acting on a fluid element:

$$d\vec{F}_{gravity} = \rho\vec{g}d\mathcal{V} \quad (II.29)$$

Total body force acting on control volume:

$$\sum \vec{F}_{body} = \int_{CV}\rho\vec{g}d\mathcal{V} = m_{CV}\vec{g} \quad (II.30)$$

**General conservation of mass**

Compensation in Reynolds transport theory (B=$m\vec{V}$ , b=$\vec{V}$):

$$\frac{d(m\vec{V})_{sys}}{dt} = \frac{d}{dt}\int_{CV}\rho\vec{V}d\mathcal{V} + \int_{CS}\rho\vec{V}(\vec{V_r}.\vec{n})dA \quad (II.31)$$

$$\sum \vec{F} = \frac{d}{dt}\int_{CV}\rho\vec{V}d\mathcal{V} + \int_{CS}\rho\vec{V}(\vec{V_r}.\vec{n})dA \quad (II.32)$$

Which can be stated as :

$$\begin{pmatrix}\text{the sum of all}\\ \text{external forces}\\ \text{acting on a CV}\end{pmatrix}=\begin{pmatrix}\text{the time rate of change}\\ \text{of the linear mouvement}\\ \text{of the contents of the CV}\end{pmatrix}+\begin{pmatrix}\text{the net flow rate of}\\ \text{linear mouvement out of the}\\ \text{control surface by mass flow}\end{pmatrix}$$

Here $\vec{V}_r = \vec{V} - \vec{V}_{CS}$ : for use in mass flow rate calculations at all locations where the fluid crosses the control surface [45].

For a fixed control volume (no motion or deformation of control volume) $\vec{V}_r = \vec{V}$

**Steady flow:**

During steady flow, the amount of mouvement within the control volume remains constant:

$$\sum \vec{F} = \int_{CS} \rho \vec{V}(\vec{V_r}.\vec{n})dA \qquad \text{(II.33)}$$

**The equation of conservation of movement for a steady flow ,tow dimensional** [47]**:**

$$(x) : u\frac{\partial u}{\partial x} + v\frac{\partial u}{\partial y} = -\frac{1}{\rho}\frac{\partial p}{\partial x} + v\left(\frac{\partial^2 u}{\partial x^2} + \frac{\partial^2 u}{\partial y^2}\right) \qquad \text{(II.34)}$$

$$(y) : u\frac{\partial v}{\partial x} + v\frac{\partial v}{\partial x} = -\frac{1}{\rho}\frac{\partial p}{\partial y} + v\left(\frac{\partial^2 v}{\partial x^2} + \frac{\partial^2 v}{\partial y^2}\right) + g\beta(T - T_0) \qquad \text{(II.35)}$$

## II-3 Numerical procedure

### II-3-1 The finite volume methods (FVM)

The finite volume method (FVM) is a discretization approach employed to solve partial differential equations, particularly those that stem from physical conservation laws. FVM utilizes a formulation based on volume integrals, where the problem is divided into a finite set of volumes to discretize the equations. This method is widely employed in the field of computational fluid dynamics for the purpose of discretizing the governing equations [48].

**Finite Volume Method in the one-dimensional case:**

- One-dimensional formulation of the Poisson Equation by the FVM:

The Poisson equation in the one-dimensional case is expressed as follows:

$$\frac{d}{dx}\left(\varepsilon\frac{d\varphi}{dx}\right) + p = 0 \qquad \text{(II.36)}$$

The field of study is divided into a finite number of nodes. Each finite volume surrounds a main node "P". The neighboring nodes are "E" on the east side and "W" on the west side. The dashed lines represent the faces of the finite volume on the east (e) and west (w) sides (Figure II.1). For a one-dimensional problem, the volume of a finite volume is [49]:

$$\Delta x \times 1 \times 1 \qquad \text{(II.37)}$$

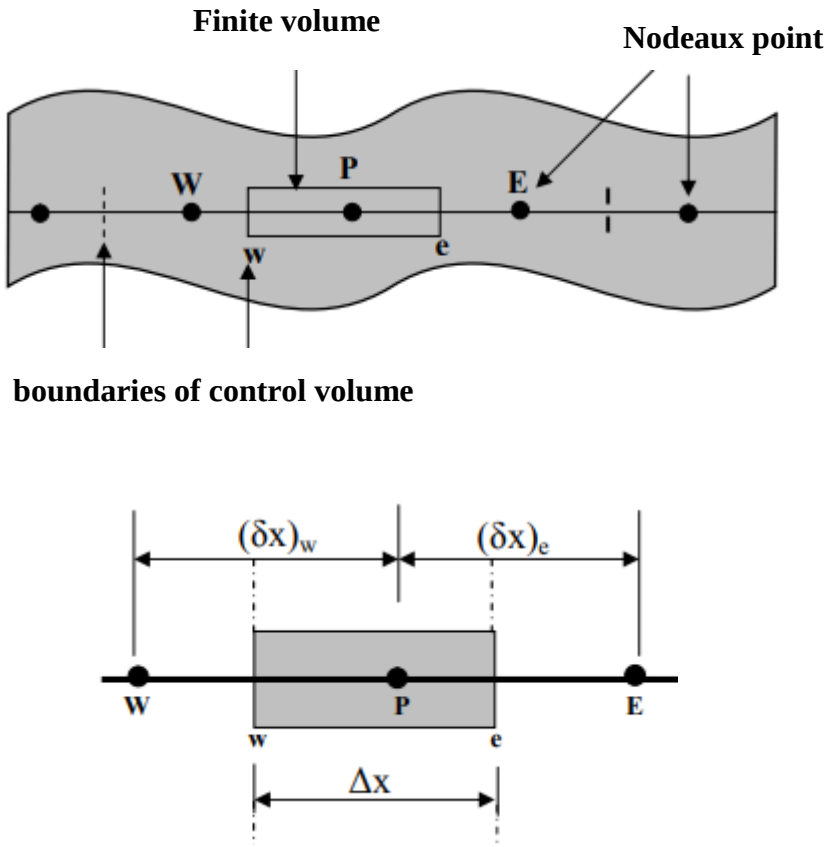


*Figure(II.5): Finite volume discretization in one-dimensional case [49].*

The equation (II.36) is integrated over the volume bounded by the faces (w,e):

$$\int_e^w \frac{d}{dx}\left(\varepsilon \frac{d\varphi}{dx}\right) dx + \int_w^e \rho dx \qquad \text{(II.38)}$$

After integration, we will have:

$$\left(\varepsilon \frac{d\varphi}{dx}\right)_e - \left(\varepsilon \frac{d\varphi}{dx}\right)_w + \int_w^e \rho dx \qquad \text{(II.39)}$$

A linear profile has been selected to express the variation of the potential φ between neighboring nodes [48]:

$$\left[\varepsilon_E \left(\frac{\varphi_E - \varphi_p}{(\delta x)_E}\right) - \varepsilon_w \left(\frac{\varphi_p - \varphi_w}{(\delta x)_w}\right)\right] + \rho_p \Delta x \qquad \text{(II.40)}$$

Such as :

$\varphi_p$: Electric potential at node P.

$\varphi_E$: Electric potential at node E.

$\varphi_w$: Electric potential at node W.

$(\delta x)_E$: The distance between nodes P and E.

$(\delta x)_w$: The distance between nodes w and P.

$\Delta x$: Finite volume length.

The final algebraic equation is written in the following form:

$$a_p\varphi_p = a_E\varphi_E + a_w\varphi_w + S \quad \text{(II.40)}$$

With:

$$a_E = \frac{\varepsilon_E}{(\delta x)_E} \quad \text{(II.41)}$$

$$a_w = \frac{\varepsilon_w}{(\delta x)_w} \quad \text{(II.42)}$$

$$a_p = a_E + a_w \quad \text{(II.43)}$$

$$S = \rho_P \times \Delta X \quad \text{(II.44)}$$

In the case of a uniform mesh:

$$\Delta x = (\delta x)_E = (\delta x)_w \quad \text{(II.45)}$$

It gives:

$$a_E = \frac{\varepsilon_E}{\Delta x} \quad \text{(II.46)}$$

$$a_w = \frac{\varepsilon_w}{\Delta x} \quad \text{(II.47)}$$

$$a_p = a_E + a_w \quad \text{(II.48)}$$

Thus, an algebraic equation is obtained that relates each main node "P" to the neighboring nodes "E" and "W". If the discretization of the domain has N nodes, we are led to solve a system of N equations with N unknowns. The resulting system will be solved using numerical resolution methods [50].

- ❖ The one-dimensional formulation of the Schrödinger Equation by the FVM:

The Schrödinger equation in the one-dimensional case can be expressed as follows:

$$-\frac{\hbar^2}{2}\left[\frac{\partial}{\partial x}\left(\frac{1}{m^*}\frac{\partial X^a}{\partial x}\right)\right] + UX^a = E^aX^a \quad \text{(II.49)}$$

Let us integrate this equation over the finite volume bounded by the interfaces (e,w):

$$-\frac{\hbar^2}{2}\left[\int_w^e \frac{\partial}{\partial x}\left(\frac{1}{m^*}\frac{\partial X^a}{\partial x}\right)\partial x\right] + \int_w^e UX^a dx = \int_w^e E^a\, X^a dx \quad \text{(II.50)}$$

Similarly to the Poisson equation, a linear profile is chosen. The integration of equation (II.50) gives [51]:

$$-\frac{\hbar^2}{2}\left[\frac{1}{m_e^*}\left(\frac{X_e^a - X_p^a}{\Delta x}\right) - \frac{1}{m_w^*}\left(\frac{X_e^a - X_p^a}{\Delta x}\right)\right] + U_pX_p^a\Delta x = E^aX_p^a\Delta x \quad \text{(II.51)}$$

The final equation:

$$a_pX_p^a = a_eX_e^a + a_wX_w^a \quad \text{(II.52)}$$

With:

$$a_e = \frac{\hbar^2}{2m_e^* \Delta x} \quad \text{(II.53)}$$

$$a_w = \frac{\hbar^2}{2m_w^* \Delta x} \quad \text{(II.54)}$$

$$a_p = a_e + a_w + (U_p - E_a)\Delta x \quad \text{(II.55)}$$

**Finite Volume Method in the two-dimensional case:**

**The bidimensional formulation of the Poisson equation by the FVM:**

The two-dimensional formulation involves dividing the study domain (Ω) into a number of finite elements. Each element contains four nodes. A finite volume surrounds each node (Figure (II.5)) [52].

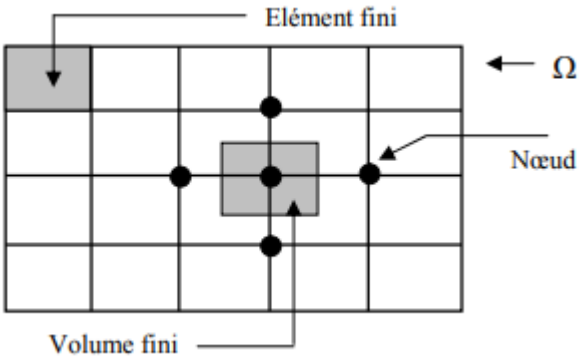


*Figure(II.6): Finite volume discretization of the study domain in the two-dimentional case. [52].*

The main node "P" is surrounded by four neighboring nodes: the North node "N", the South node "S" (in the y direction), and the West node "W", the East node "E" (in the x direction).

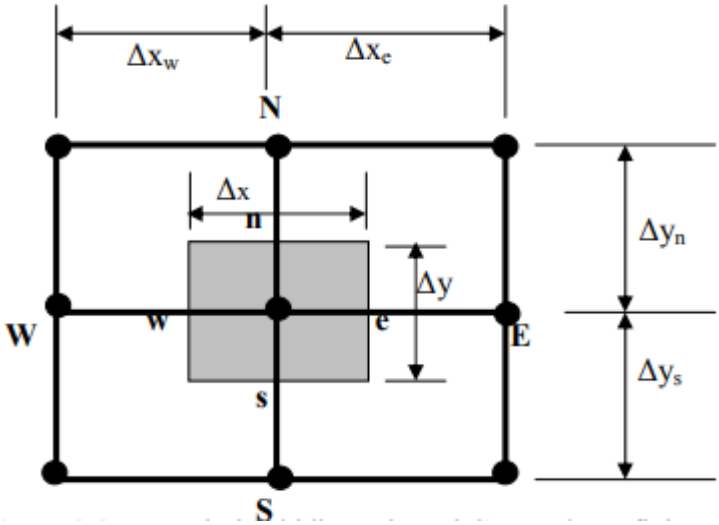


*Figure(II.7): Two-dimensional description of a finite volume [52].*

❖ The Poisson equation in the two-dimensional case is expressed as:

$$\frac{\partial}{\partial x}\left(\varepsilon\frac{\partial\varphi}{\partial x}\right)+\frac{\partial}{\partial y}\left(\varepsilon\frac{\partial\varphi}{\partial y}\right)=-\rho \quad \text{(II.56)}$$

By integrating over the corresponding finite volume at node P, we find:

$$\int_w^e\int_s^n\frac{\partial}{\partial x}\left(\varepsilon\frac{\partial\varphi}{\partial x}\right)dxdy+\int_w^e\int_s^n\frac{\partial}{\partial y}\left(\varepsilon\frac{\partial\varphi}{\partial y}\right)dxdy=\int_w^e\int_s^n-\rho\,dxdy \quad \text{(II.57)}$$

The integration of the left-hand side of the equation (II.57) over the finite volume bounded by (e, w, s, n) is:

$$\int_w^e\int_s^n\frac{\partial}{\partial x}\left(\varepsilon\frac{\partial\varphi}{\partial x}\right)dxdy+\int_w^e\int_s^n\frac{\partial}{\partial y}\left(\varepsilon\frac{\partial\varphi}{\partial y}\right)dxdy=\left[\left(\varepsilon\frac{\partial\varphi}{\partial x}\right)_e-\left(\varepsilon\frac{\partial\varphi}{\partial x}\right)_w\right]\Delta y+\left[\left(\varepsilon\frac{\partial\varphi}{\partial y}\right)_n-\left(\varepsilon\frac{\partial\varphi}{\partial y}\right)_s\right]\Delta x \quad \text{(II.58)}$$

The integration of the right-hand side gives:

$$\int_w^e\int_s^n-\rho\,dxdy=\rho_p\Delta x\Delta y \quad \text{(II.59)}$$

We suppose that:

$$S=\rho_p\Delta x\Delta y \quad \text{(II.60)}$$

From another side about the left-hand side a linear profile has been selected to express the potential variation φ between neighboring nodes. The obtained result is solely composed of nodal values:

$$\left(\varepsilon\frac{\partial\varphi}{\partial x}\right)_e=\varepsilon_e\left(\frac{\varphi_e-\varphi_p}{\Delta x_e}\right) \quad \text{(II.61)}$$

$$\left(\varepsilon\frac{\partial\varphi}{\partial x}\right)_w=\varepsilon_w\left(\frac{\varphi_p-\varphi_w}{\Delta x_w}\right) \quad \text{(II.62)}$$

$$\left(\varepsilon\frac{\partial\varphi}{\partial y}\right)_n=\varepsilon_n\left(\frac{\varphi_n-\varphi_p}{\Delta y_n}\right) \quad \text{(II.63)}$$

$$\left(\varepsilon\frac{\partial\varphi}{\partial y}\right)_s=\varepsilon_s\left(\frac{\varphi_p-\varphi_s}{\Delta y_s}\right) \quad \text{(II.64)}$$

Then The final algebraic equation is written in the following form [53]:

$$a_p\varphi_p=a_e\varphi_e+a_w\varphi_w+a_s\varphi_s+a_n\varphi_n+S \quad \text{(II.65)}$$

With:

$$a_e=\varepsilon_e\frac{\Delta y}{\Delta x_e} \quad \text{(II.66)}$$

$$a_w=\varepsilon_w\frac{\Delta y}{\Delta x_w} \quad \text{(II.67)}$$

$$a_n=\varepsilon_n\frac{\Delta x}{\Delta y_n} \quad \text{(II.68)}$$

$$a_s=\varepsilon_s\frac{\Delta x}{\Delta y_s} \quad \text{(II.69)}$$

$$a_p = a_e + a_w + a_s + a_n \quad \text{(II.70)}$$

❖ The two-dimensional formulation of the Schrödinger equation using the FVM:

$$\frac{-\hbar^2}{2}\left(\frac{\partial}{\partial x}\left(\frac{1}{m^*}\frac{\partial X^a}{\partial x}\right)+\frac{\partial}{\partial y}\left(\frac{1}{m^*}\frac{\partial X^a}{\partial y}\right)\right)+UX^a = E^aX^a \quad \text{(II.71)}$$

Let us integrate this equation over the finite volume bounded by the interfaces (e, w, s, n):

$$\frac{-\hbar^2}{2}\left[\int_w^e\int_s^n\left(\frac{\partial}{\partial x}\left(\frac{1}{m^*}\frac{\partial X^a}{\partial x}\right)+\frac{\partial}{\partial y}\left(\frac{1}{m^*}\frac{\partial X^a}{\partial y}\right)\right)dxdy\right]+\int_w^e\int_s^n UX^a dxdy = \int_w^e\int_s^n E^a X_p^a\, dxdy \quad \text{(II.72)}$$

Similarly to the Poisson equation, a linear profile is selected. Integrating the left-hand side of equation (II.72) gives:

$$-\frac{\hbar^2}{2}\left[\frac{1}{m_e^*}\left(\frac{X_e^a-X_p^a}{\Delta x_e}\right)\Delta y-\frac{1}{m_w^*}\left(\frac{X_p^a-X_x^a}{\Delta x_w}\right)\Delta y+\frac{1}{m_n^*}\left(\frac{X_n^a-X_p^a}{\Delta y_n}\right)\Delta x-\frac{1}{m_s^*}\left(\frac{X_p^a-X_s^a}{\Delta y_s}\right)\Delta x\right]+U_pX_p^a\Delta x\Delta y \quad \text{(II.73)}$$

By the integration of the right-hand side of the equation we got:

$$\int_w^e\int_s^n E^a X_p^a\, dxdy = E^aX_p^a\Delta x\Delta y \quad \text{(II.74)}$$

The final algebraic equation is expressed in the following form [54]:

$$a_pX_p^a = a_eX_e^a + a_wX_w^a + a_nX_n^a + a_sX_s^a \quad \text{(II.75)}$$

With:

$$a_e = \frac{\hbar^2}{2m_e^*}\frac{\Delta y}{\Delta x_e} \quad \text{(II.76)}$$

$$a_n = \frac{\hbar^2}{2m_n^*}\frac{\Delta x}{\Delta y_n} \quad \text{(II.77)}$$

$$a_w = \frac{\hbar^2}{2m_w^*}\frac{\Delta y}{\Delta x_w} \quad \text{(II.78)}$$

$$a_s = \frac{\hbar^2}{2m_s^*}\frac{\Delta x}{\Delta y_s} \quad \text{(II.79)}$$

$$a_p = a_e + a_w + a_n + a_s + (U_P - E_a)\Delta x\Delta y \quad \text{(II.80)}$$

**II-4 Presentation of Gambit software**

The software Gambit (Geometry and Mesh Building Intelligent Toolkit) is a 2D/3D mesh generator and a pre-processor that allows for meshing the geometry domains of a CFD problem. It can generate structured or unstructured meshes in Cartesian, polar, cylindrical, or axisymmetric coordinates. It is capable of creating complex meshes in two or three dimensions with mesh types of rectangles or triangles. The mesh generation options in Gambit provide flexibility in choices. The geometry can be decomposed into multiple parts to generate a structured mesh. Alternatively, Gambit automatically generates an unstructured mesh suitable for the constructed geometry type. With mesh verification tools, defects are easily detected.

It can be used to build a geometry and generate a mesh for it, and potentially, a geometry from another CAD software can be imported into this pre-processor. It generates *.msh files for Fluent.

**Gambit**

↓

Geometry And Mesh Building Intelligent Toolkit

**An all-in-one preprocessor designed for CFD analysis:**

**-Import and construct geometric shapes:**

- using ACIS solid modeling capabilities .
- using STEP , IGES,… import and cleanup even modification of imported data.

**-Mesh generation of all Fleunt solvers (FIPAD,POLYFLOW ?...):**

- Structured and unstructured hexahedral , tetrahydral , pyramidand prisms.

**- Mesh quality examination.**

**-Boundray zone assignement.**

### II-4-1 Gambit initiation

The sequence of steps for utilizing the Gambit application is as follows:

**/Fluent.Inc/ntbin/ntx86/Gambit.exe**

It is possible to create a shortcut on the taskbar. If there is an execution issue, delete all ***.lok** files in the directory **/Fluent.Inc/ntbin/ntx86** and restart **Gambit.exe** [57]**.**

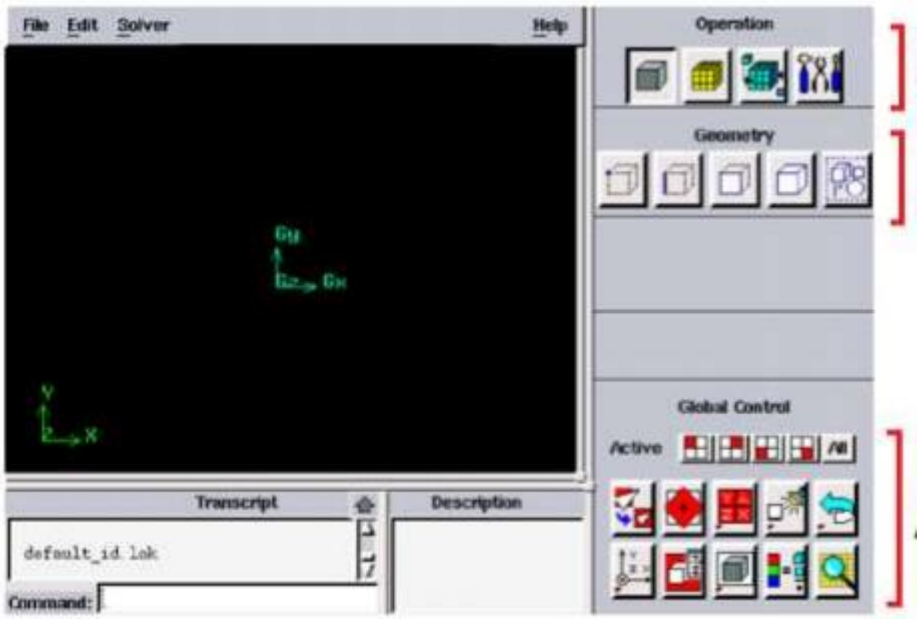


*Figure(II.8): Gambit's graphical user interface.*

### II-4-2 Features of Gambit

The Gambit software encompasses three main functions: defining the geometry of the problem (constructing it if the geometry is simple or importing it from CAD software), meshing and its verification, and defining the boundaries (types of boundary conditions) and calculation domains. If the geometry is designed using CAD software (such as Solidworks or CATIA), it is advisable to import files in ACIS *.sat format, and it is often necessary to clean up the geometry.

In the top right corner, various operations that can be performed in this software are displayed, as shown in Figure (II.8).

* The initial operation involves geometry. This menu enables the creation of volumes, surfaces, lines, and points. It is also possible to modify imported geometries.

*The second operation is the meshing of the geometry. This menu allows for the meshing of volumes and surfaces, as well as the discretization of lines.

*The third operation enables the definition of boundary conditions and fluid domains.

*The fourth button functions as a tool menu.

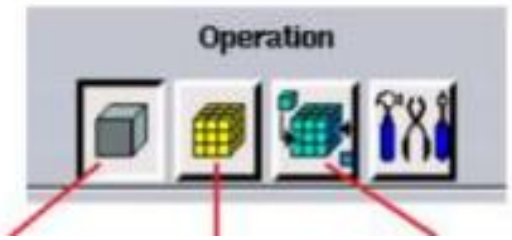


**Geometry construction.** **Geometry meshing.** **The definition of boundaries and fluid domains .**

*Figure(II.9): The main functions of Gambit's general menu.*

### II-4-3 Description of the mesh menu

The mesh menu is comprised of five buttons, as depicted in the table provided :

*Table(II.1): Description of mesh menu commands.*

| *Commande* | Couches limites | Segment | Faces | Volume | Groupe |
|---|---|---|---|---|---|
| *Symbole* |  |  |  |  |  |

The main mesh menu description, as shown in Figure (II.10), is as follows:

1. Creation and modification of a boundary layer type mesh.

2. Size of the first cell.

3. Mesh expansion factor.

4. Number of specific mesh lines.

5. Mesh type (4 specific mesh types are available).

6. Single-line mesh.

7. Application of a double ratio that increases point density either on the sides or in the center of lines.

8. Use of a ratio for the mesh.

9. Choice of mesh option: number of nodes or interval size between the two.

10. Face mesh.

11. Smoothing of deformed meshes.

12. Choice of mesh type: Tri, Quad.

13. If the option checked, creation of a regular mesh according to the parameters below; if not, create a mesh from nodes defined on the edges.

14. Volume mesh.

15. Smoothing of deformed meshes.

16. Choice of mesh type: Tetra, Hex.

17. If option checked, creation of a regular mesh according to the parameters below. If not, creation of a mesh from nodes defined on the edges.

When specifying a mesh element type, each element is linked to a schema (Table II.2) and a mesh type (Table 2-4):

*Table(II.2): The schema specification for the elements of the face gambit.*

| Option | Description |
|---|---|
| Quad | Specify that the mesh only contains quadrilateral elements |
| Tri | Specify that the mesh only contains triangular elements. |
| Quad/tri | Specify that the mesh is composed of quadrilateral elements but may contain triangular elements. |

*Table(II.3): Mesh element type specification in Gambit for faces.*

| Option | Description |
|---|---|
| Map | Create a regular and structured mesh. |
| Submap | Divide a complex geometric surface into a more regular region and create a structured mesh in each region. |
| Pave | Develop an unstructured mesh |
| Tri primitive | Divide a three-sided face into three quadrilateral regions and create a structured mesh in each region. |

## II-5 The fluent Software

Fluent is a general purpose package for modeling fluid flow and heat transfer. It is used for simulation, visualization, and analysis of fluid flow, heat and mass transfer, and chemical reactions.

Fleunt is the world's largest provider of commercial computational fluid dynamics software and services. Fleunt offers general-purpose CFD software for a wide range of industrial applications, along with highly automated, specifically focused packages.

Fluent provides complete mesh flexibility, including the ability to solve your flow problems using unstructured meshes that can be generated about complex geometries with relative ease. Supported mesh types include 2D triangular/quadrilateral, 3D, ect.

Fluent also allows you to refine or coarsen your grid based on the flow solution.

When starting the fluent software, we must choose the dimensions of the calculation domain (2D or 3D), and the precision that the software must use single precision or double precision.


*Figure(II.10): Choice of dimensions and precision.*

**The main simulation steps under FLUENT are the following**

1. Importing geometry (*.msh)

« File>Read>Case ».

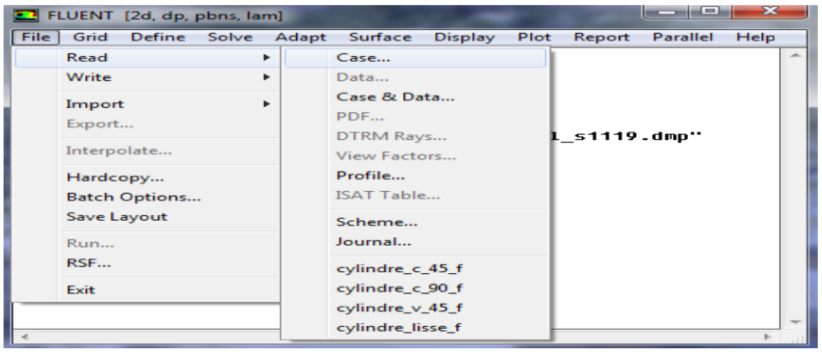


*Figure(II.11): Importing geometry.*

2. Che cking the imported mesh

« Grid>Check »

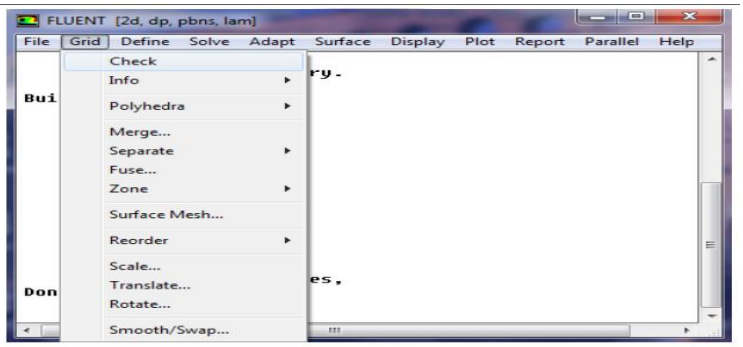


*Figure(II.12): Cheking the mesh.*

### 3. Smoothing the mesh (Smooth and swap the grid)

To be assured of the quality of the mesh, we must smooth it, we click on the "Smooth" button, then on the "Swap" button. The operation will be repeated until Fluent declares to us that zero faces are "swapped".

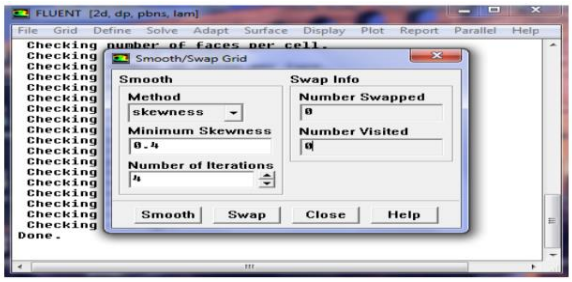


*Figure(II.13): Smoothing the mesh.*

4.Verification of dimensions and of units

« Grid>Scale »

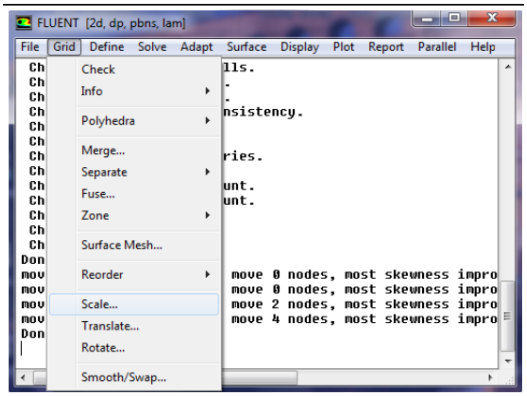


*Figure(II.14): Verification of dimension and units.*

5. Choice of the solver and the state of the flow

« Define>Models>Solver »

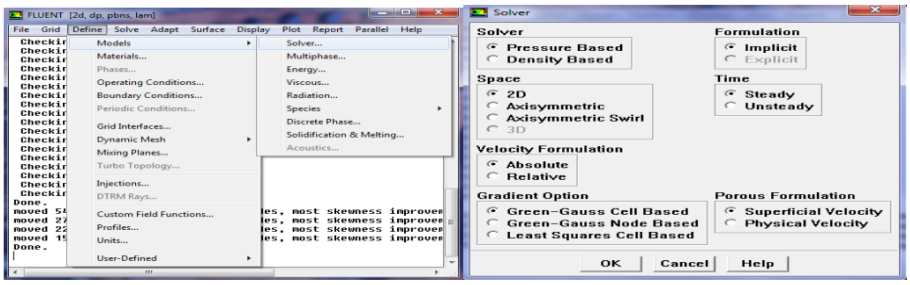


*Figure(II.15): Choice of the solver.*

### II-5-1 Verification of the Mesh

A collection of points representing the flow field, where the equations of fluid motion (and temperature, if relevant) are calculated.

Check the scale of the mesh by selecting the scale button under mesh in general on the task page.

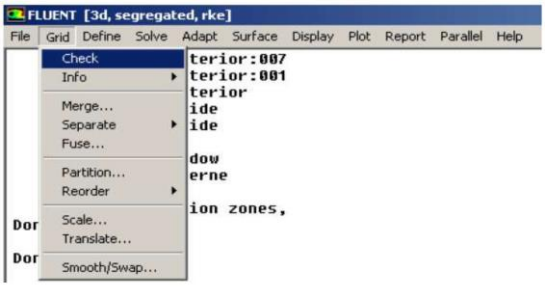


*Figure(II.16): Verification of mesh on fluent.*

### II-5-2 Boundary Conditions

In this step, we must introduce the values of the boundary conditions (velocity wall, pressure inlet, mass flow inlet, ect.).

Define → Boundary Conditions

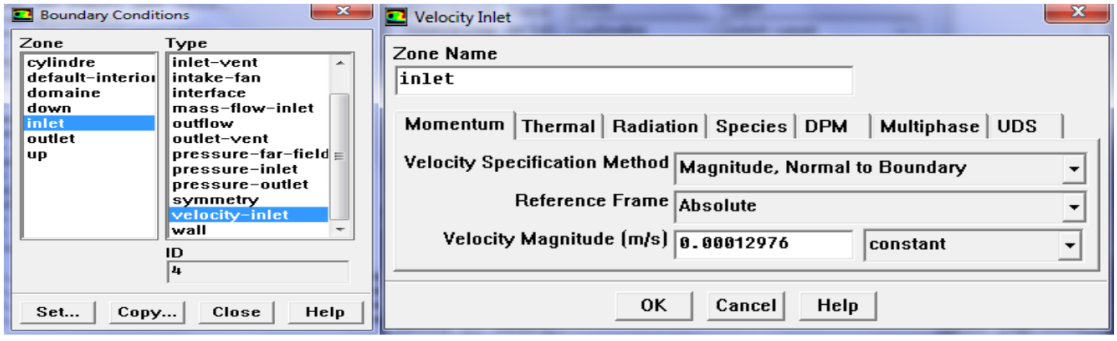


*Figure(II.17): Entry speed.*

### II-6 Turbulance

The enhancement technique of heat transfer through corrugated walls is a crucial feature in the design of compact heat exchangers, as demonstrated by numerous empirical studies and numerical investigations reported in the literature. The physical process of enhancing heat transfer arises from the fact that the corrugated shape of the surface disrupts the boundary layer formed and allows for continuous replacement of the fluid near the solid wall. Therefore, the optimal solution is to minimize pressure drop while maximizing heat transfer.

### II-6-1 Definition of a Turbulence Phenomenon

Turbulence refers to the state of a fluid, liquid, or gas in which the velocity at any point has a swirling character (vortices whose size, location, and orientation constantly vary). Turbulent flows are therefore characterized by a very disorderly appearance, unpredictable behavior, and the existence of numerous spatial and temporal scales. Such flows occur when the source of kinetic energy that sets the fluid in motion is relatively intense compared to the viscosity forces that the fluid opposes to move. Conversely, laminar flow refers to the regular character of a flow. The discovery and study of turbulence are very ancient; for example, they were made by Leonardo da Vinci. Osborne Reynolds, who revived the study of turbulence at the end of the 19th century. The complex behavior of turbulent flows is mostly approached through statistical methods. It can be considered that the study of turbulence is part of statistical physics. To express the fact that in a flow, inertia forces dominate viscosity forces, a suitably chosen Reynolds number must exceed a certain threshold. For the study of turbulence in natural environments, it is preferable to use the Richardson number rather than the Reynolds number, as the latter assumes the fluid density to be constant, which is not true for compressible fluids. A classically highlighted property of turbulent flow lies in a process called an energy cascade. The division of large vortices into smaller vortices allows for energy transfer from large scales to small scales. This process is limited by the effect of molecular dissipation, which prevents too-significant velocity variations. In practice, this allows the punctual transfer of small swirling structures (which merge) towards one or more larger structures.

### II-6-2 General characteristics of turbulence

Turbulence can be characterized by the following points:

- Temporal and spatial fluctuations of large amplitude in all physical quantities (velocity components, pressure, etc.).
- Vortical structures of greatly different characteristic sizes are nested within each other and interact with each other.
- Each physical quantity has an energy spectrum (i.e., the spectrum of the square of the fluctuation) that is continuous and tends towards zero at high wave numbers (i.e., at the smallest spatial scales).
- Persistence of turbulence. Once initiated, a turbulent flow tends to persist; it continues to produce vortices to replace those that have dissipated. This is particularly true for turbulent flows with walls and for shear layers; this persistence is not related to the instability mechanisms of T-S waves in laminar flow.
- Mixing in turbulent flow is much more efficient than mixing in laminar flow.

### II-7 Trapezoidal Rule

It is a numerical integration technique used to approximate the value of a definite integral of a function. This method is considered simple and effective for calculating integrals where analytical solutions may be difficult or impossible to obtain. The trapezoidal rule is commonly used in engineering and science to address problems that require numerical integration[55].

### II-7-1 Theoretical Basic

In the trapezoidal rule, the interval over which the function is to be integrated is divided into $n$ equal-length subintervals. Each consecutive pair of points forms a trapezoid (a geometric shape resembling a grid). The idea is to approximate the area under the curve by summing the areas of these trapezoids.

### II-7-2 Mathematical Formula

Formally, if $f(x)$ is the function to be integrated over the interval $[a, b]$, and if we divide this interval into $n$ subintervals of width $h$ then the estimation of the integral using the trapezoidal rule is given by the following formula:

$$\int_a^b f(x)dx \approx \frac{h}{2}[f(x_0) + 2f(x_1) + 2f(x_2) + \cdots + 2f(x_{n-1}) + f(x_n)] \quad \text{(II.81)}$$

where:

- $x_0 = a$ and $x_n = b$ .
- $h$ is the length of each subinterval and is calculated by the equation $h = \frac{b-a}{n}$ .

This formula is derived by approximating each subinterval with a trapezoid, hence the name of the method. As the number of subintervals ( $n$ ) increases, the accuracy of the approximation increases, as the trapezoids become closer to the curve of the integrated function.

## II-8 The standard model ( k $-\varepsilon$)

The $\mathbf{k}-\boldsymbol{\varepsilon}$ model is one of the most widely used turbulence models in modeling turbulent flows. It is employed in the field of computational fluid dynamics (CFD) and numerical analysis of flows to predict turbulent flow behavior in various engineering and industrial applications.

The variable **k** represents the turbulent kinetic energy, measuring the amount of kinetic energy present in the turbulent flow per unit volume. On the other hand, the variable $\boldsymbol{\varepsilon}$ represents the rate of dissipation of this turbulent kinetic energy, which is the rate at which kinetic energy is converted into thermal energy due to turbulent flow.

### II-8-1 The transport equations of the standard k-ε model

The **k-ε** turbulence model is a viscosity model, where it is assumed that Reynolds stresses are proportional to the gradients of the mean velocity (Boussinesq hypothesis).

We obtain the following transport equations:

$$\frac{\partial}{\partial t}(\rho k) + \frac{\partial}{x_i}(\rho k U_i) = \frac{\partial}{\partial x_j}\left[\left(\mu + \frac{\mu_t}{\sigma_k}\right)\frac{\partial k}{\partial x_j}\right] + G_k + G_b - \rho\varepsilon - S_k \quad \text{(II.82)}$$

$$\frac{\partial}{\partial t}(\rho \varepsilon) + \frac{\partial}{x_i}(\rho \varepsilon U_i) = \frac{\partial}{\partial x_j}\left[\left(\mu + \frac{\mu_t}{\sigma_k}\right)\frac{\partial \varepsilon}{\partial x_j}\right] + G_{1\varepsilon}\,\frac{\varepsilon}{k}(G_k + C_{3\varepsilon}G_b) - C_{2\varepsilon}\rho\frac{\varepsilon^2}{k} + S_\varepsilon \quad \text{(II.83)}$$

In these equations:

$\mu_t$: The proportionality constant representing turbulent viscosity.

$G_k$: Represents the generation of turbulent kinetic energy due to gradients in the mean velocity.

$G_b$ : The generation of turbulent kinetic energy resulting from turbulence dissipation.

$C_{1\varepsilon}$ ; $C_{2\varepsilon}$; $C_{3\varepsilon}$ : Empirical constants.

$\sigma_k$ et $\sigma_\varepsilon$: Prandtl numbers for k and ε respectively.

$S_k$, $S_\varepsilon$: Source terms.

With:

$$\mu_t = \rho C_\mu \frac{k^2}{\varepsilon} \quad \text{(II.84)}$$

Where $C_\mu$ is an empirical constant.

**Model constants**

$C_{1\varepsilon} = 1.44$ , $C_{2\varepsilon} = 1.92$ , $C_\mu = 0.09$ , $\sigma_k = 1.0$ , $\sigma_\varepsilon = 1.3$

These default values were determined based on experiments with water and air, as well as fundamental turbulent shear flow studies.

## II-9 The conlusion

In conclusion, the effective integration of GAMBIT and FLUENT software with the finite volume method provides a powerful approach to solving the conservation equations for mass, motion, energy.

This combination allows for accurate modeling of complex physical phenomena, yielding reliable numerical results. Utilizing these tools requires a deep understanding of the underlying physical principles and modeling techniques, but in return, it offers significant capability to study and optimize a wide range of engineering problems.

# CHAPTER III
# Finding and Analysis

## III-1 Introduction

In this chapter, we present and discuss the results of the simulation of convection in our cylindrical, horizontal geometry, and two pipes at different inclinations (α = 30 deg, 60 deg) without and with control elements at three different positions (x = 50, 200, and 400 mm). We will also analyze the results of the pipe with a control element at x = 50 mm .

## III-2 Problem Statement

The aim of this study is to explore flow control to enhance (intensify) heat transfer in cylindrical tubes using vortex generators (the passive method). The effect of inclination on the heat transfer rate will also be analyzed. The geometry under study is a copper cylindrical tube, 500 mm in length, with an inner diameter of 10 mm and a wall thickness of 1 mm. Fins in the form of circular rings, 1 mm thick and 1 mm wide, are inserted along the inner surface of the tube at various positions. The working fluid is water flowing initially in laminar and subsequently in turbulent flow with Reynolds numbers of 1500 and 15000, respectively.

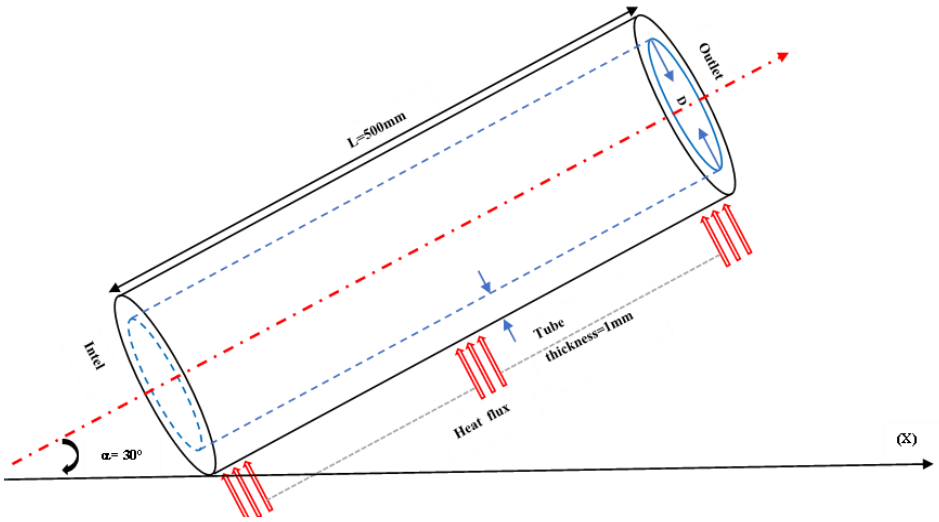


*Figure( III.1): Draw a smooth pipe inclined at 30 degrees.*

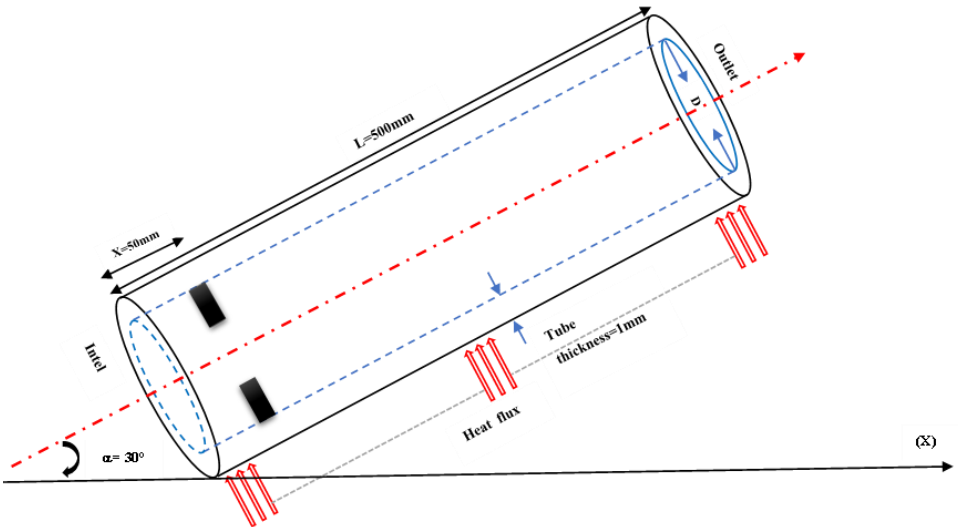


*Figure( III.2): A pipe inclined at 30 degrees with a control element (x = 50mm).*

### III-4 Mesh selection

Mesh selection is a crucial step in numerical simulation. It ensures the independence of the solution obtained from the mesh used and avoids numerical errors. A mesh independence study was conducted to choose the most appropriate mesh for our simulation. Mesh independence is assessed by the small variation of the average convective heat transfer coefficients.

For this purpose, five different meshes were tested, their details are mentioned in Table (III.1) Calculations were performed for a smooth vertical pipe for laminar flow with a Reynolds number Re = 1500 and for an inlet temperature and pressure Ti = 293 K and Pi = 1 bar, respectively, with a wall heat flux density of $q = 10000\ W/m^2$. The heat transfer coefficients calculated using the numerical procedure for each chosen mesh are also presented in Table (III.2).

It can be observed that, starting from the third mesh (M3), the value of the convective heat transfer coefficient remains constant. Therefore, meshes (M1) and (M2) are not suitable, as there is an unjustified variation in the exchange coefficient. Finally, mesh (M3) was selected for this numerical study because it yields the same results as meshes (M4) and (M5) but with a smaller size see (Table III.1). For the chosen mesh (M3) illustrated in Figure (III.3) and Figure (III.4), a total of 270,000 elements were generated in the fluid zone and 30,000 elements in the solid zone.

*Table (III.1): Details of the various meshes tested.*

| Meshes | Fluid | Solid |
|---|---|---|
| M1 | 30000 | 10000 |
| M2 | 120000 | 20000 |
| M3 | 270000 | 30000 |
| M4 | 30000 | 10000 |
| M5 | 120000 | 20000 |

*Table (III.2): Average convective heat transfer coefficient for different meshes.*

| Meshes | M1 | M2 | M3 | M4 | M5 |
|---|---|---|---|---|---|
| $\bar{h}$ [w/m²K] | 944.9524 | 908.4986 | 913.217 | 913.216 | 913.215 |

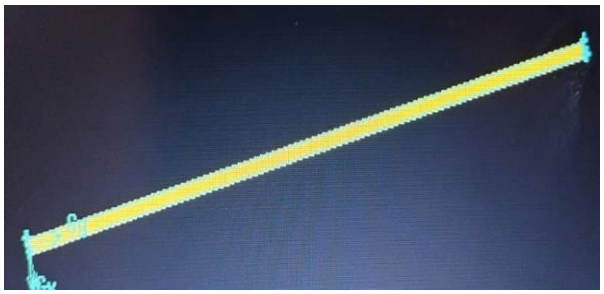

*Figure( III.3): The chosen inclined mesh.*


*Figure( III.4): The chosen horizontal mesh.*

### III-5 Method for calculating the Nusselt number

The approach adopted to determine the Nusselt number is as follows:

The conduit is subdivided into several sections as shown in Figure (III.5)

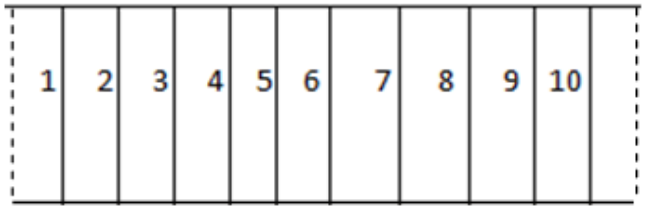


*Figure( III.5): Subdivision of the conduit section for the calculation of the local Nusselt number.*

In each section, the heat flux density and the wall temperature are determined.

To calculate the reference temperature (average mixture temperature) in each section, the equation (III.1) formula is used:

$$T_m(x) = \frac{\int_{A_c} \rho u C_p T dA_c}{\dot{m}\, C_p} \qquad \text{(III.1)}$$

In each section, the local convective heat transfer coefficient is calculated using the formula of equation (III.2), and the local Nusselt number by equation (III.3):

$$h(x) = \frac{q_p(x)}{T_p(x) - T_m(x)} \qquad \text{(III.2)}$$

$$Nu(x) = \frac{h(x).x}{\lambda} \qquad \text{(III.3)}$$

The average values of Nu are determined from the local values.

### III-6 Flow control for enhancing heat transfer

#### III-6-1 Smooth pipe

Before examining flow control using heat transfer enhancement techniques (vortex generators), we will analyze the effect of inclination on heat transfer. Three pipes will be used:

The first is a smooth horizontal pipe (α = 0 deg), the second has an inclination of α = 30 deg, and the third has an inclination of α = 60 deg. The boundary conditions for the results presented below are for water flow in the studied tube with an inlet temperature and pressure of 293 K and 1 bar, respectively. A constant heat flux of 10 $kW/m^2$ is imposed on the external surface of the tube.

Two flow regimes have been studied: laminar flow with an inlet Reynolds number Re = 1500 corresponding to a velocity u = 0.1507 m/s, and turbulent flow with a Reynolds number Re = 15000 corresponding to an inlet velocity u = 1.507m/s.

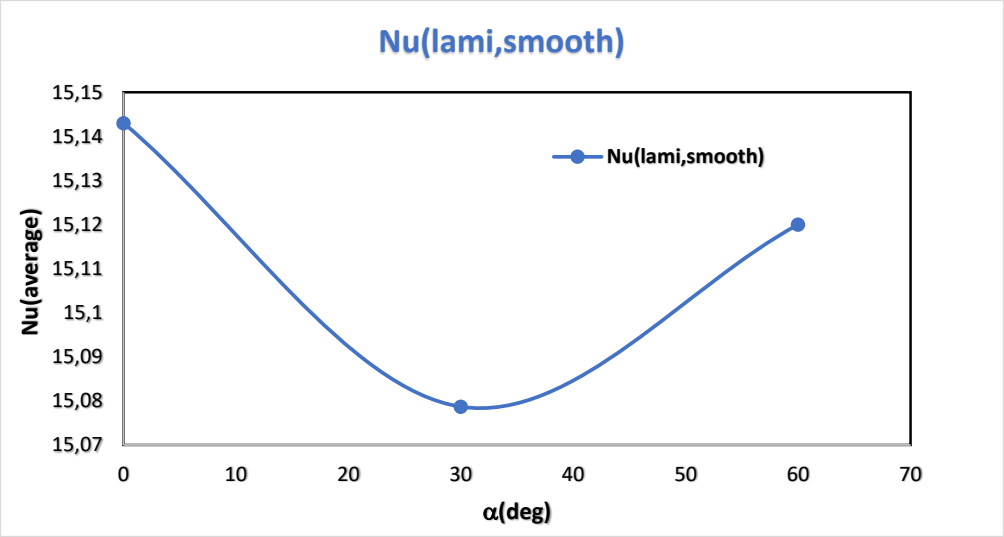


*Figure( III.6): Variation of the average Nusselt number in a smooth pipe at different inclinations for laminar regime (Re=1500).*

The value of the average Nusselt number for a laminar regime is approximately equal in the three tubes (horizontal tube (α= 0 deg), inclined tube (α = 30 deg), and (α= 60 deg)). There is no improvement in heat transfer for the laminar regime.

Figure(III.7) shows the variation of the average Nusselt number in a smooth pipe:

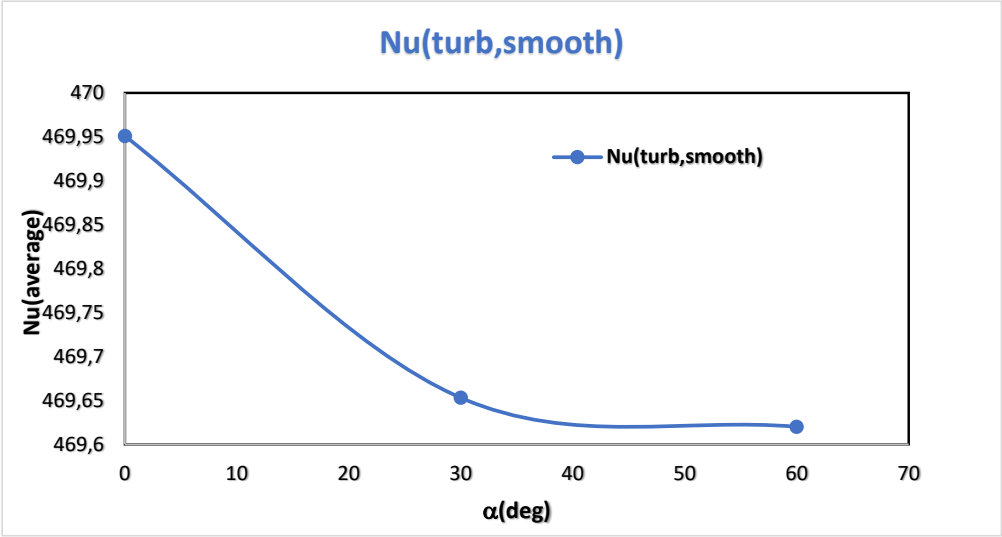


*Figure( III.7): Variation of the average Nuseelt number in a smooth pipe at different inclinations for a turbulent regime (Re=15000).*

The value of the average Nusselt number for a turbulent regime is approximately equal in the three tubes (horizontal tube (α= 0 deg), inclined tube (α =30deg), and (α=60deg)). There is no improvement in heat transfer for the turbulent regime.

The value of the average Nusselt number for the turbulent regime is higher than the value of the average Nusselt number for the laminar regime for the horizontal pipe, inclined pipe (α = 30 deg), and inclined pipe (α= 60 deg).

The average Nusselt number for the turbulent regime in the inclined smooth pipes is higher than the Nusselt number for the laminar regime in the inclined smooth pipes.

### III-6-1-1 Temperature fields for a smooth horizontal pipe

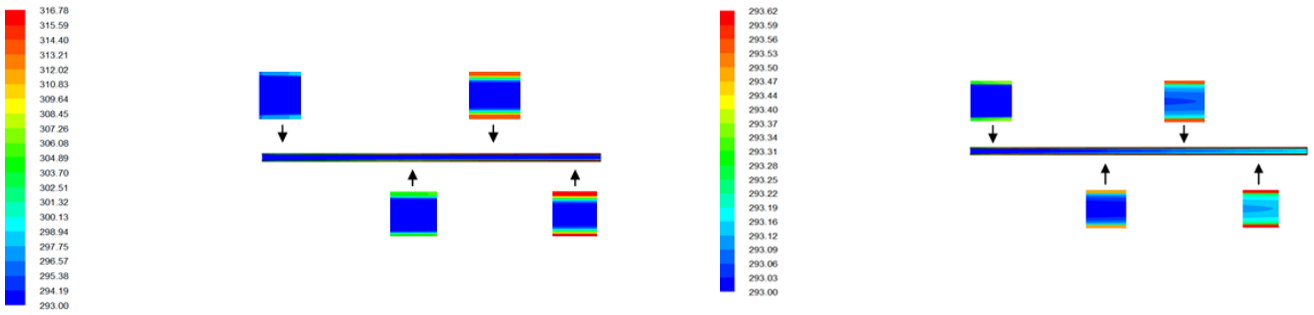

(a) (b)

*Figure( III.8): Presents the temperatures fields for a smooth horizontal pipe: a-Laminar regime (Re=1500) b-Turbulent regime (Re=15000).*

### III-6-1-2 Velocity fields for a smooth horizontal pipe

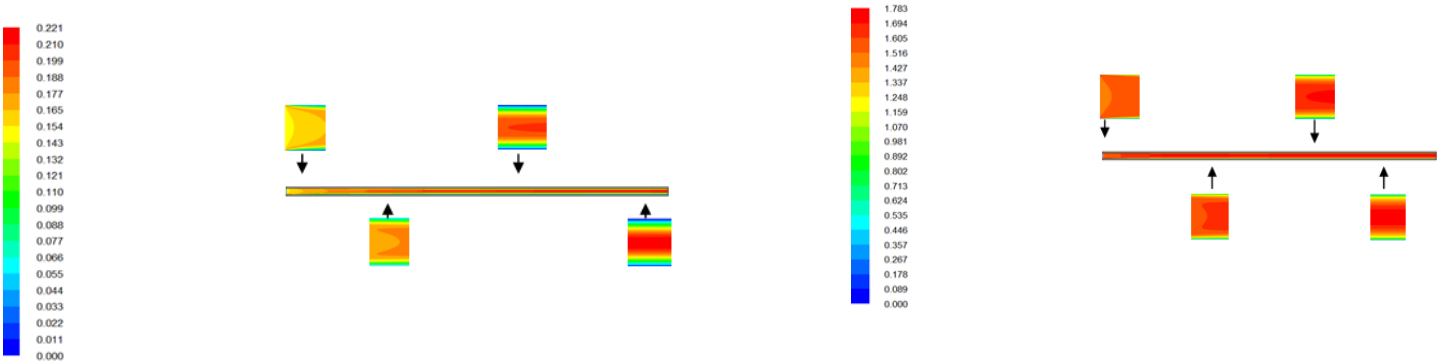


(a) (b)

*Figure( III.9): Presents the velocity fields for a smooth horizontal pipe : a-Laminar regime(Re=1500),b-Turbulent regime (Re=15000).*

Figure (III.10) illustrates the change in average Nusselt number in a pipe with control elements at various positions (x=50, 200, and 400 mm) at different inclinations (α =0 deg, α = 30 deg, and α = 60 deg) for a laminar flow regime (Re = 1500).

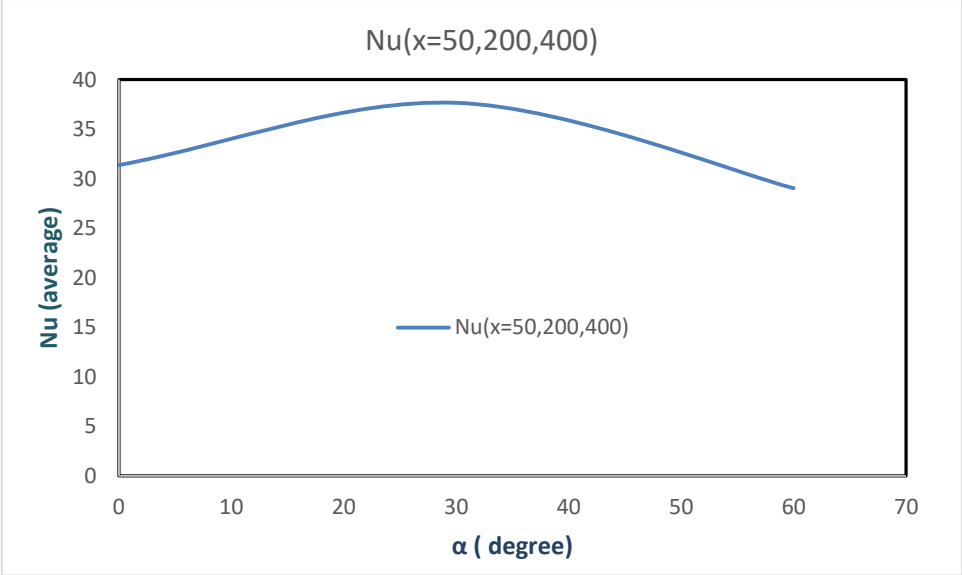


*Figure( III.10): The average Nusselt number variation in a pipe with control elements at multiple positions(x=50,200,400mm) at different inclinations for a laminar flow regime (Re=1500).*

The average Nusselt number at an angle α = 30 deg is greater than the average Nusselt number for horizontal conduits (α = 0 deg) and inclined conduits α = 60 deg. To enhance heat transfer in inclined tubes, it is preferable to use a tube inclined at 30 deg by adding control elements at three different positions (x = 50, 200, and 400 mm).

Figure (III.11) illustrates the change in average Nusselt number in a Smooth pipe and a pipe with control elements at multiple positions (x=50, 200, and 400 mm) at various inclinations (α = 0 deg, α = 30 deg, and α = 60 deg) for a laminar flow regime (Re = 1500).

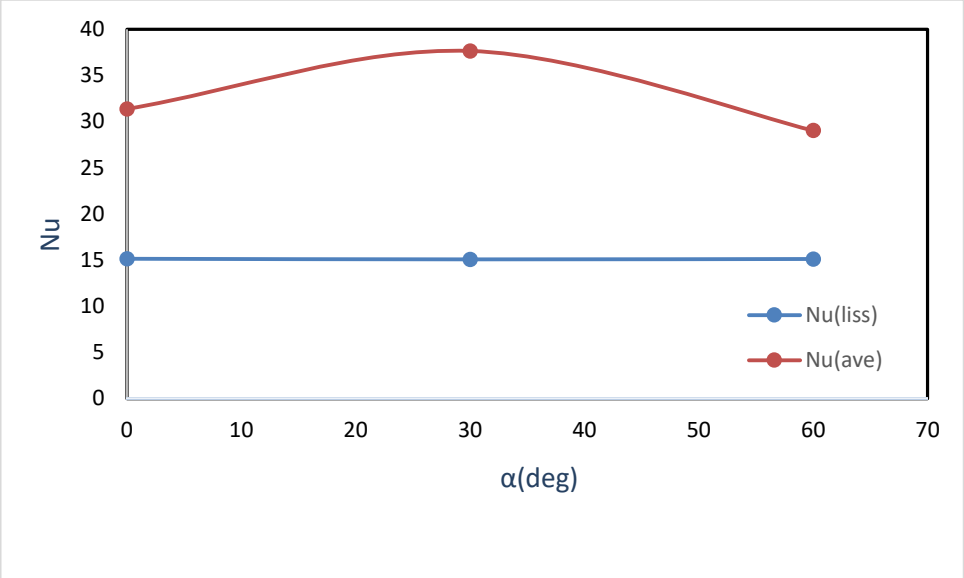


*Figure( III.11): The change in average Nusselt number in a smooth pipe and a pipe with control elements (Re=1500).*

The average Nusselt number for horizontal pipe (α= 0 deg), inclined pipe (α= 30 deg), and inclined pipe (α=60 deg) with control elements at different positions (x= 50, 200, and 400 mm) is higher than the average Nusselt number for smooth horizontal pipe (α= 0 deg), smooth inclined pipe (α = 30 deg), and smooth inclined pipe (α = 60 deg). To enhance heat transfer, it is preferable to use inclined tubes equipped with control elements at different positions (x= 50, 200, and 400 mm) instead of using smooth inclined tubes as they do not increase the heat transfer rate. The optimal angle is 30 deg.

Figure (III.12) illustrates the variation of the average Nusselt number in a smooth pipe and a pipe with control elements at multiple positions (x=50, 200, and 400 mm) at different inclinations (α = 0 deg, α= 30 deg, and α= 60 deg) for a turbulent flow regime (Re = 15000).

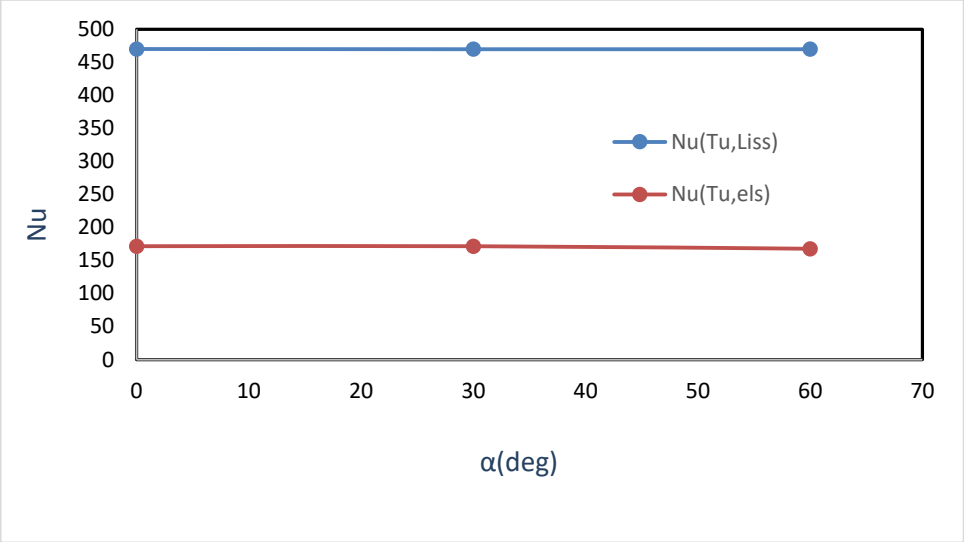


*Figure( III.12): Ilustrates the variation of the average Nusselt number in a smooth pipe and a pipe with control elementss at different inclinations for a turbulent flow regime (Re=15000).*

For the turbulent regime, the average Nusselt number for inclined pipes with control elements at multiple positions (x = 50, 200, and 400 mm) is lower than the average Nusselt number for smooth inclined pipes. In the turbulent regime, the addition of control elements at multiple points (x = 50, 200, and 400 mm) decreases the heat transfer rate of inclined tubes compared to smooth inclined tubes.

Figure (III.13) illustrates the variation of the local convection coefficient in a smooth horizonta pipe (α = 0 deg) and a pipe with a control element at the position x = 50 mm with an inclination of α = 30 deg for a laminar regime (Re = 1500).

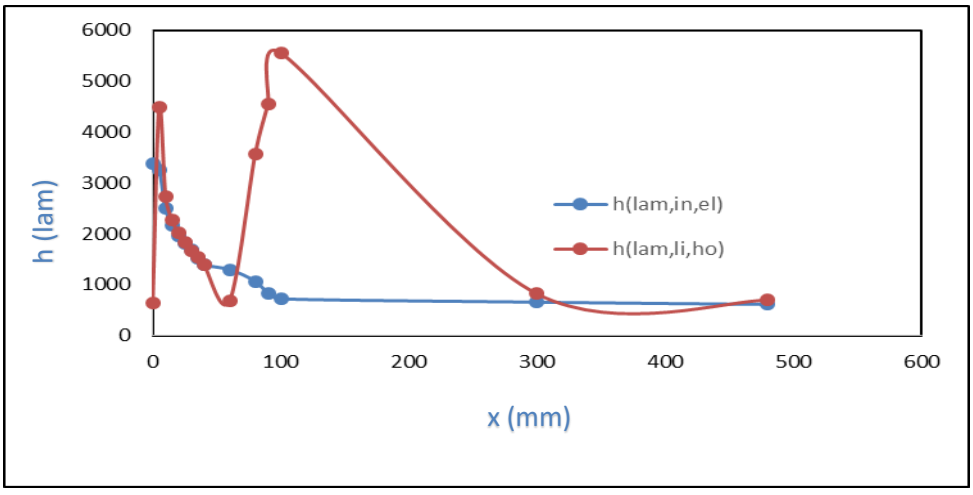


*Figure( III.13): The local convective coefficient variation in a smooth horizontal pipe (alpha=0deg) and a pipe with a control element at position x=50mm withan inclination (alpha=30 deg) investigated forr a laminar flow regime (Re=1500).*

The local convection coefficient for the inclined pipe (α = 30 deg) with a control element at position x = 50 mm is higher than the local convection coefficient for the smooth horizontal pipe (α = 0 deg) at most distances. However, the local convection coefficient for the inclined pipe (α = 30 deg) with a control element at position x = 50 mm is lower than the local convection coefficient for the smooth horizontal pipe (α = 0 deg) only at the point x = 480 mm.

The addition of a control element at the distance x = 50 mm improves the heat transfer in the inclined pipe (α = 30 deg) for laminar flow (Re = 1500).

Figure (III.14) shows the velocity field for an inclined pipe (α = 30 deg) with control elements at positions x = 50, 200, and 400 mm for laminar flow (Re = 1500).

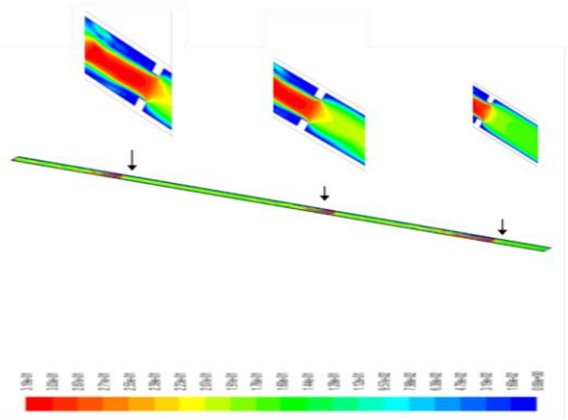

*Figure( III.14): Illustrates the velocity field for inclined flow (alpha=30deg) with control elements(x=50,200,400mm) for a laminar regime (Re=1500).*

Figure (III.15) illustrates the temperature field for an inclined pipe (α = 30 deg) with control elements (x = 50, 200, and 400 mm) for a laminar flow regime (Re = 1500).

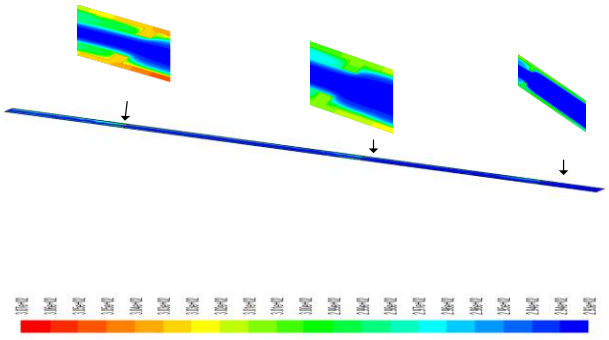

*Figure( III.15): The temperature field for an inclined pipe (alpha =30deg) with control elements (x=50,200,400mm) for a laminar flow regime (Re=1500).*

Figure (III.16) illustrates the change in local convection coefficient in a horizontal pipe (α =0 deg) with control elements at (x = 50, 200, and 400 mm) and a pipe with a control element at position x = 50 mm at an inclination (α = 30 deg) for laminar flow (Re = 1500).

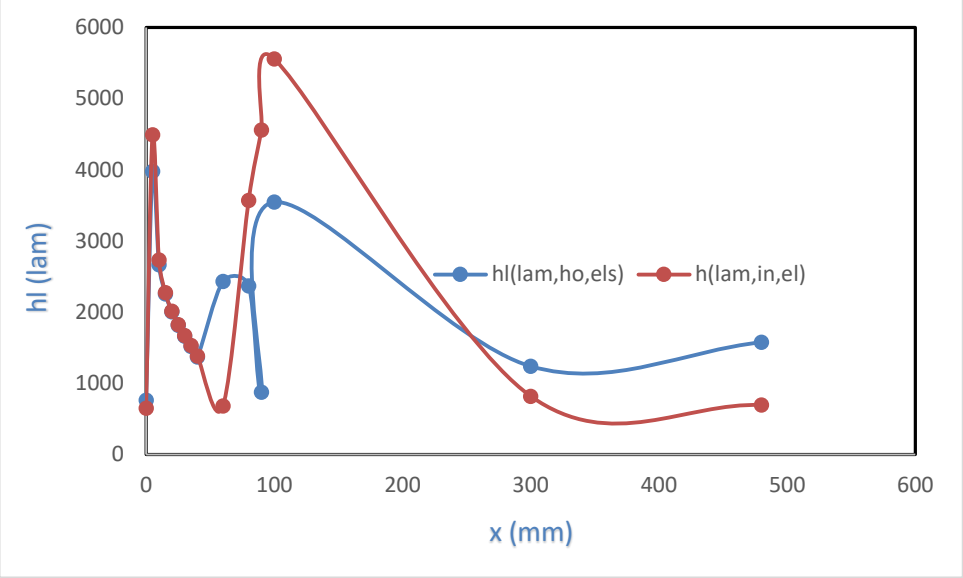


*Figure( III.16): The local head loss in a horizontal pipe with control elements and inclined pipe (alpha=30deg) with a control element at x=50mm.*

The local convection coefficient in the inclined pipe (α = 30 deg) with a control element at x =50 mm is higher than the local convection coefficient in a horizontal pipe with control elements at (x = 50, 200, and 400 mm) at several distances except at the distance of x = 300 to 480 mm.

Using an inclined tube (α = 30 deg) with a single control element at x = 50 mm will be better than using a horizontal tube with control elements at (x = 50, 200, and 400 mm). This is because the inclined tube will allow for faster liquid displacement, which will increase the heat exchange.

Figure (III.17) shows a comparison of the globally calculated Nusselt number in three smooth pipes numerically. The first one is horizontal, the second one is inclined with (α = 30 deg), and the third one is inclined with (α = 60 deg) in laminar flow with a Reynolds number Re = 1500. The Shah and London correlation for thermally developed region, constant wall heat flux, and laminar flow gives:

$$\mathrm{Nu} = 1.953\left(\mathrm{R_e} \times \mathrm{P_r} \times \frac{\mathrm{D}}{\mathrm{L}}\right)^{0.33} \qquad \text{(III.4)}$$

Applicable to:

$$(\mathrm{R_e} \times \mathrm{P_r} \times \mathrm{D/L}) > 33.3 \qquad \text{(III.5)}$$

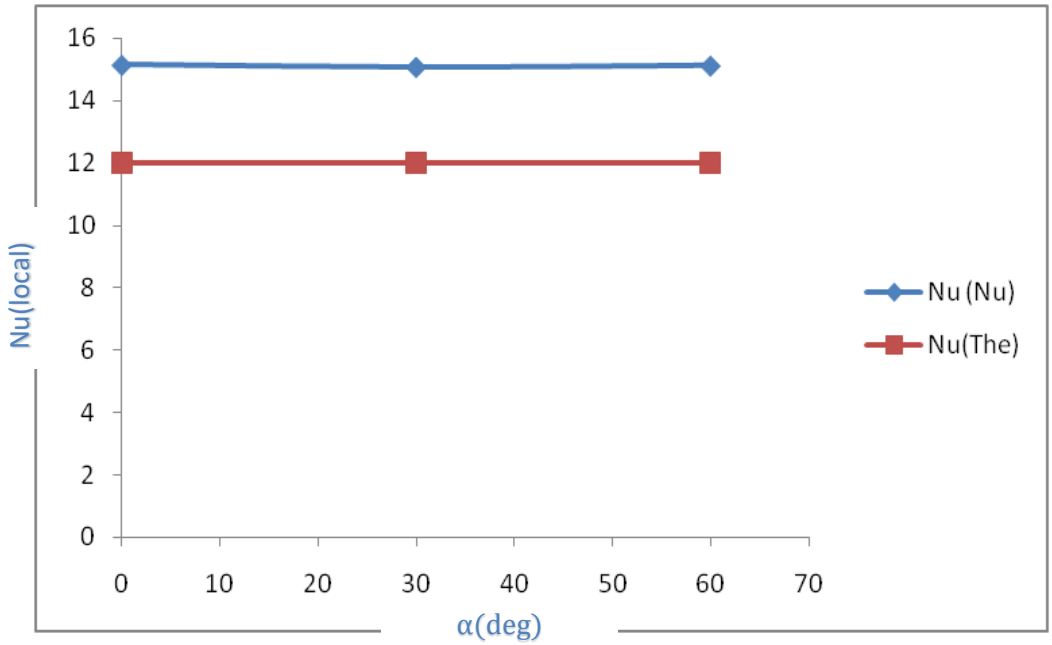


*Figure( III.17): Illustrates the comparison of the numerically calculated overall Nusselt number in three smooth pipes and theoretical overall Nuselt number for a Laminar regime.*

The globally calculated Nusselt values obtained numerically for three different type

s of smooth pipes (horizontal, inclined with α = 30 deg, and inclined with α = 60 deg) and the theoretically calculated Nusselt values using the Shah and London correlation for laminar flow (Re = 1500) exhibit a high degree of similarity.

## III-7-Conclusion

The numerical study of enhancing heat transfer in cylindrical conduits (tubes) by combining tube inclination with passive enhancement techniques is investigated, these tubes can serve as absorbers for solar concentrators or be part of heat exchangers.

The findings of this study demonstrate the possibility of controlling the flow within the conduits to enhance heat transfer by attaching control elements at various positions on the internal surface of the conduits. For further improvement in heat transfer, the aforementioned technique can be combined with tube inclination.

We used Fluent software based on the finite volume method for numerical simulation. Our study's results focused on the variations of local and global convection coefficients, the global Nusselt number, and the temperature and velocity fields for different Reynolds numbers (Re = 1500 and 15000), including cases with and without control elements for a horizontal reference case. Additionally, we studied different inclination angles (α = 0, 30, 60 degrees).

Our study has highlighted the importance of vortex generators in enhancing heat transfer. While typically there is no improvement in heat transfer efficiency when considering horizontal (α= 0 degrees) and inclined tube cases at 30 and 60 degrees, the presence of vortex generators in inclined

tubes can significantly enhance heat transfer. Vortex generators create swirling flows that disrupt the boundary layer, thereby promoting better heat transfer rates by increasing the mixing of fluid layers.

Our findings revealed that the introduction of fins led to a decrease in the heat transfer rate in the turbulent system for all inclinations, while the heat transfer rate increased in the pressurized flow. Furthermore, we determined the optimal angles that maximize heat transfer. In the turbulent regime, the addition of control elements at multiple points (x = 50, 200, and 400 mm) resulted in a decrease in the heat transfer rate compared to smooth inclined tubes. Based on our calculations, we concluded that the best angle for the laminar regime in inclined pipes with control elements (x = 50, 200, and 400 mm) is 30 degrees.

# General Conclusion

## General conclusion

In this study, we focused on conducting numerical investigations of forced convection to enhance heat transfer to a Newtonian fluid (specifically water) using forced convection with vortex generators in inclined pipes. We examined both laminar and turbulent flows by introducing a vortex generator at the inlet of inclined cylindrical pipes with limited thickness, where the fluid is incompressible and Newtonian (water). The outer walls of these pipes were subjected to a constant surface heat flow. To model this physical problem, we utilized the equations of conservation of mass, momentum, and energy in the Cartesian coordinate system.

To perform the calculations, we employed fluent software that is based on the finite volume method for numerical simulation. The results of our study focused on the variations of the local and global convection coefficients, the global Nusselt number, and the temperature and velocity fields for different Reynolds numbers (Re = 1500 and 15000). We explored several configurations, including cases with and without control elements, for a horizontal reference case. Additionally, we considered various inclinations ($\alpha$ = 0, 30, 60 degrees).

The results showed that integrating vortex generators significantly affects heat transfer rates. The introduction of fins increased heat transfer in laminar flows but caused a decrease in turbulent flows for all inclination angles. Furthermore, the study indicated that placing control elements at various positions within the pipes can help determine the optimal angles to maximize heat transfer efficiency. For the laminar regime with control elements positioned at multiple points (x = 50, 200, and 400 mm), the inclination angle of 30 degrees was the most effective.

This study highlights the potential to improve fluid flow within inclined pipes through the strategic use of vortex generators and control elements. It demonstrates the feasibility of manipulating the flow within the conduits to enhance heat transfer by placing control elements at various positions on the internal surface of the conduits.

These techniques can be effectively applied in systems such as solar concentrators and heat exchangers, where enhanced heat transfer is crucial. Future research could explore the integration of different passive and active techniques to optimize heat transfer in various applications.

## References


[1] M. Bernadr, mechanics of fluids, eighth éd., 2006, pp. 12-35.

[2] P. F. a. McDonald's, Introduction of fluid mecanics, 8 éd., 2011.

[3] N. Hall, «phases of matter,» [En ligne]. Available: https://www.grc.nasa.gov/www/k-12/airplane/state.html. [Accès le 20 12 2023].

[4] R. K. Bansal, Fluid Mechanics, 1983.

[5] R. Rajput, A Textbook of Fluid Mechanics, LPSPE éd., 1998.

[6] M.-W. Frank, Fuids mechanics, seventh éd., 2011, pp. 20-31.

[7] I. Moghtada Mobedi · Gamze Gediz, Fundamentals of heat transfer, 2023, pp. 16-29.

[8] D. Robert w fox and philip j.pritchard and alan T.Mc, introduction to fluid mechanics, 6th éd., 2004, pp. 35-54.

[9] H. A. Joseph, fluid mechanics, second éd., 2019.

[10] D. P. D. T. L. B. A. S. L. Frank P. Incropera, Fundamentals of Heat and Mass Transfer, 7th éd., 2011, pp. 65-70.

[11] J. Daniel R.Flynn and Bradley A and Peavy, thermal conductivity Held at the National Bureau of Standards, Gaithersburg, Maryland November 13-16, 1967, Gaithersburg, pp. 13-16.

[12] R. Stephen, university of central arkansas, 2001.

[13] P. J. P. R. W. F. A. T. McDonald, Introduction to Fluid Mechanics, 8 éd., 2011, p. 64.

[14] «Fluid Flow Classifications,» [En ligne]. Available: https://courses.ansys.com/wp-content/uploads/2020/06/What_is_a_Fluid-Lesson3-Flow_Classification-Handouts.pdf. [Accès le 2 1 2024].

[15] M. Frank, Viscous fluid flow, 3 éd., 2005, pp. 20-50.

[16] J. S. Marshall, Inviscid incompressible flow, 2001, pp. 10-30.

[17] K. R, Heat and mass transfer, 2016, pp. 413-414.

[18] Y. A. Ç. a. A. J. GHAJAR, Heat and mass transfer, 4 éd., 2018, pp. 380-388.

[19] T. L. B. A. S. L. F. P. I. و. D. P. DeWitt, Fundamentals of Heat and Mass Transfer, 5 éd., 2011, p. 636.

[20] «Intro to Forced Convection,» [En ligne]. Available: https://courses.ansys.com/wp-content/uploads/2021/02/S1LT4C2L1_Handout_NT.pdf. [Accès le 5 2 2024 ].

[21] «Intro to Laminar Boundary Layer Theory,» [En ligne]. Available: https://courses.ansys.com/wp-content/uploads/2020/08/Laminar-Boundary-Layer-Theory-Lesson1-Handout.pdf. [Accès le 25 2 2024].

[22] Y. A. C. a. J. M. Cimbala, Fluid Mechanics: Fundamentals and Applications, 3 éd., 2013.

[23] G. M.S, «Forced Convection,» [En ligne]. Available: https://www.slideshare.net/slideshow/forced-convection/47242472. [Accès le 20 3 2024].

[24] D. Varudharajan, «Boundary layer and heat exchangers,» [En ligne]. Available: https://www.slideshare.net/vgopinathme/boundary-layer-and-heat-exchangers. [Accès le 30 3 2024].

[25] A. Mills, Heat transfer , Prentice hall, New Jersey, 1999.

[26] S. W. L. E. Brid R.B, Transport phenomena, wiley new york, 2007.

[27] Y. A. McGraw-Hill, Heat and mass transfer, 3rd éd., new york, 2007, p. from 450 to 700.

[28] R. P.Chabra, CRC handbook of thermal engineering, 2nd éd.

[29] A. D. a. J. R. a. A. Aziz, Introduction to thermal and fluid engineering.

[30] A. S. ,. F. P. a. D. P. Theodore L.Bergman, Fundamentals of heat and mass transfer, 2006.

[31] H. A. M. N. N.-G. a. B. S. S. Tabatabaeikia, «Heat transfer enhancement by using different types of inserts,» 2014.

[32] S. Jamshed, «A Brief Review of Techniques of Thermal Enhancement in Tubes,» 2023.

[33] V. O. Orhan Keklikcioglu, Heat Transfer - Models, Methods and Applications, IntechOpen, Éd., 2018, p. Ch. 10.

[34] a. o. L. Léal, «An Overview of Heat Transfer Enhancement Methods and New Perspectives: Focus on Active Methods Using Electroactive Materials,» vol. 61, pp. 505-524, 2013.

[35] I. J. o. E. D. a. R. (IJEDR), Éd.«Heat Transfer Enhancement In Pipe With Passive Enhancement Technique,» vol. 5, 2017.

[36] S. S. Mousavi Ajarostaghi, «A review of recent passive heat transfer enhancement methods engeries,» 2022.

[37] R. L. W. N. Y. Kim, Enhanced Heat Transfer, T. a. Francis, Éd., New York, 2005.

[38] «Review of Heat Transfer Augmentation Through Different Passive Intensifier Methods2278,» vol. 1, pp. 14-21, 2012.

[39] J. P. Sagar, «A review on heat transfer enhancement methods for a heat exchanger,» 2022.

[40] J. Adem, «Vortex generator model and its application to flow control journal of aircraft,» vol. 42, n° %16, pp. 1486-1491, 2005.

[41] O. L"ogdberg, Vortex generators and turbulent boundray layer separation control, 2006.

[42] R. L.Webb, enhancement heat transfer, 1994.

[43] S. Kalogirou, Solar Energy engineering and systems, 2009.

[44] F. M.White, Fluid Mechanics, 7 éd., 2011.

[45] Y. A. Ç. J. M. CIMBALA., Fluid Mechanics, 2013, pp. 172-178.

[46] Y. A. Ç. A. J. GHAJAR, Heat and Mass Transfer, FIFTH éd., 2014, pp. 11-14.

[47] Z. HADDAD, *Etude des effets d'un nanofluide sur un écoulement de convection naturelle dans une cavité, thèse de doctorat, Université des Sciences et de Technologie Houari Boumediene,* 2014.

[48] F. M. L. M. M. Darwish, The Finite Volume Method in Computational Fluid Dynamics, 2015 .

[49] T. G. H. Robert Eymard, Finite Volume Methods, 2019, p. 12.

[50] Z. M. V. Amal Bergam, «Estimations a posteriori d'un schéma de volumes finis pour un problème non linéaire,» vol. 95, pp. 599-624, 2003.

[51] F. KHOMH, *Volumes Finis Mixtes Hybrides et Ecoulements en milieu poreux,* 2003.

[52] B. R. B. ,. K. a. S. Acharya, «Pressure-based finite-volume methods in computational fluid dynamics,» 2007.

[53] R. G. T. e. H. R. EYMARD, Finite volume methods. Handbook of numerical analysis,, vol. 7, 2000, pp. 713-1018.

[54] F. M. L. D. M. e. a. « MOUKALLED, The finite volume method. Springer International Publishing, 2016.

[55] R. a. F. J. Burden, Numerical Analysis, 10 éd., 2016.